© 2019. Published by The Company of Biologists Ltd | Journal of Cell Science (2019) 132, jcs229849. doi:10.1242/jcs.229849

RESEARCH ARTICLE

Retinoblastoma protein represses E2F3 to maintain Sertoli cell quiescence in mouse testis

Emmi Rotgers[1,2], Sheyla Cisneros-Montalvo[1,2], Mirja Nurmio[1,2] and Jorma Toppari[1,2,*]

ABSTRACT

Maintenance of the differentiated state and cell cycle exit in adult Sertoli cells depends on tumor suppressor retinoblastoma protein (RB, also known as RB1). We have previously shown that RB interacts with transcription factor E2F3 in the mouse testis. Here, we investigated how *E2f3* contributes to adult Sertoli cell proliferation in a mouse model of Sertoli cell-specific knockout of *Rb* by crossing these mice with an *E2f3* knockout mouse line. In the presence of intact RB, *E2f3* was redundant in Sertoli cells. However, in the absence of RB, *E2f3* is a key driver for cell cycle re-entry and loss of function in adult Sertoli cells. Knockout of *E2f3* in Sertoli cells rescued the breakdown of Sertoli cell function associated with *Rb* loss, prevented proliferation of adult Sertoli cells and restored fertility of the mice. In summary, our results show that RB-mediated repression of E2F3 is critical for the maintenance of cell cycle exit and terminal differentiation in adult mouse Sertoli cells.

KEY WORDS: RB, E2F3, Cell cycle, Spermatogenesis, Sertoli cell

INTRODUCTION

Sertoli cells are highly differentiated somatic cells that control and support sperm development in the adult testis. As the fetus develops, Sertoli cells are the first cell type to undergo male sex differentiation as a result of *SRY* gene activation (Capel, 2017; Kashimada and Koopman, 2010; Mirza et al., 2006) and Sertoli cell proliferation drives testicular organogenesis and expansion of the testis cords (Ungewitter and Yao, 2013). Sertoli cells gradually cease proliferation and terminally differentiate during puberty (Vergouwen et al., 1991). Adequate Sertoli cell proliferation is important for fertility; Sertoli cell number determines sperm output in the adult, as a single Sertoli cell can support only a finite number of germ cells (Ranganathan et al., 1994; Rebourcet et al., 2017).

Sertoli cells were long thought to permanently exit the cell cycle as they terminally differentiate in the mouse (Tarulli et al., 2012). However, based on data from different species, it has been suggested that Sertoli cells are in a state of continuous cell cycle repression rather than terminally differentiated (Tarulli et al., 2012). First, Sertoli cell proliferation is reactivated during the reproductive season in seasonal breeders such as the Djungarian hamster, where Sertoli cell numbers fluctuate depending on the photoperiod and associated gonadotropin levels (Tarulli et al., 2006). Second, when adult mouse or human Sertoli cells are removed from their physiological environment to *in vitro* culture conditions, some of them can re-enter the cell cycle (Ahmed et al., 2009). Sertoli cells are maintained in a non-proliferative state in adulthood by the retinoblastoma protein (RB, also known as RB1) tumor suppressor protein (Nalam et al., 2009; Rotgers et al., 2014). Loss of *Rb* in Sertoli cells (SC-*Rb*KO mouse line) results in reactivation of Sertoli cell proliferation in adult mice, which ultimately leads to spermatogenic failure as a result of Sertoli cell dysfunction (Nalam et al., 2009; Rotgers et al., 2014). We showed that shRNA-mediated *in vivo* knock-down of transcription factor E2F3 could ameliorate the testicular phenotype of SC-*Rb*KO mice (Rotgers et al., 2014).

A key function of RB is to regulate the E2F transcription factors, which are crucial players in the control of cell cycle, apoptosis and differentiation (reviewed in Chen et al., 2009). The classical view of RB–E2F-mediated cell cycle control is that upon mitogenic signaling, cyclin-dependent kinases (CDKs) inactivate RB by phosphorylation, which results in the release of E2F and activation of genes required for cell cycle progression. The E2F protein family has eight members, traditionally classified as transcriptional activators (E2F1–E2F3a) and repressors (E2F3b–E2F8) (Chen et al., 2009). These classifications are not as clear-cut *in vivo*; the activator E2Fs can switch to repressors during differentiation through forming complexes with RB family proteins (Chong et al., 2009). All the E2Fs share the same consensus DNA-binding sequence (Zheng et al., 1999) and there is considerable functional redundancy between family members (Tsai et al., 2008).

Adult mouse Sertoli cells express two E2F family members, E2F3 and E2F4 (El-Darwish et al., 2006); however, two *E2f3* isoforms are transcribed from the same gene locus through the use of an alternative promoter (Adams et al., 2000; He et al., 2000; Leone et al., 2000). E2F3a is classified as a transcriptional activator, while the shorter E2F3b isoform is a transcriptional repressor (Adams et al., 2000). E2F3a and E2F3b can have opposing roles in regulating cell fate *in vivo*, but their function is dependent on the cellular context. In neural progenitor cells E2F3a promotes differentiation, while E2F3b promotes progenitor fate and supports the expansion of the neural precursor colony (Julian et al., 2013). However, in myotubes E2F3b activates the expression of genes required for differentiation (Asp et al., 2009). Furthermore, increased *E2f3* activity in the absence of *Rb* leads to defects in both proliferation and apoptosis in lens and neuronal cell lineages (Chong et al., 2009; Ziebold et al., 2001). Thus, the function of E2F3 is highly dependent on the cell lineage in question and their RB expression status.

We investigated the contribution of E2F3 RB-mediated cell cycle control in Sertoli cells by interbreeding the SC-*Rb*KO (*Amh*-cre;$Rb^{flox/flox}$) strain with the $E2f3^{flox/flox}$ strain to achieve a simultaneous conditional knockout of *Rb* and *E2f3* in Sertoli cells (Lécureuil et al., 2002; Marino et al., 2000; Wu et al., 2001). In adult males, a complete loss of *E2f3* rescued the testicular dysfunction caused by *Rb* deficiency. However, in the absence of *Rb*, even one

[1]Institute of Biomedicine, Research Centre for Integrative Physiology and Pharmacology, University of Turku, Turku 20520, Finland. [2]Department of Pediatrics, Turku University Hospital, Turku 20520, Finland.

*Author for correspondence (jorma.toppari@utu.fi)

S.C.-M., 0000-0001-5667-4846; J.T., 0000-0003-2228-334X

Received 14 January 2019; Accepted 11 June 2019

Journal of Cell Science (2019) 132, jcs229849. doi:10.1242/jcs.229849

copy of intact *E2f3* gene was able to drive adult Sertoli cell proliferation, coupled with a depletion of spermatogenesis and a disruption of the blood–testis barrier.

RESULTS

E2F3 expression was induced in Sertoli cells upon cell cycle exit

E2F3 has been shown to be expressed in adult mouse Sertoli cells and spermatogonia (El-Darwish et al., 2006), but the expression pattern of the two isoforms, E2F3a and E2F3b, in the postnatal testis was unknown.

We analyzed both E2F3 protein and mRNA expression using immunohistochemistry and RNA *in situ* hybridization on postnatal day (P)6, P10, P20 and P40 testes to assess the expression pattern during the major events in postnatal Sertoli cell development (Fig. 1). On P6, Sertoli cells are actively proliferating, on P10 they gradually begin to exit the cell cycle, by P20 Sertoli cell proliferation has ceased and in P40 mouse testis full spermatogenesis is reached. Surprisingly, E2F3a protein was expressed in only a subpopulation of Sertoli cells on P6 (Fig. 1A, black arrowheads), but the proportion of E2F3a-positive Sertoli cells increased gradually as the animals matured. By P20 all the Sertoli cells were positive for E2F3a (Fig. 1A). To analyze whether E2F3a expression in immature Sertoli cells was associated with a non-proliferative state as a sign of commitment to terminal differentiation, consecutive sections of P6 and P10 testes were stained for E2F3a and KI67 (Fig. 1A, black double arrows and KI67 in inset). There was no correlation between KI67 and E2F3a staining, as the E2F3a-positive Sertoli cells were seen to be both KI67-positive and -negative (Fig. 1A, black and red double arrows, respectively). As expected, the signal using an antibody against both E2F3 isoforms (E2F3ab) followed a similar pattern in Sertoli cells as the E2F3a-specific antibody (Fig. 1B, red arrowheads show E2F3ab-negative cells, black arrowheads show E2F3ab-positive cells). However, in spermatogonia the E2F3a isoform was not detected at either P6 or P10 (Fig. 1A, yellow arrowheads), and only the antibody against both isoforms (E2F3ab) gave a positive signal (Fig. 1B, orange arrowheads). The expression pattern of *E2f3a* mRNA, and of both *E2f3a* or *E2f3b* mRNA detected by a non-isoform-specific probe (E*2f3ab* mRNA hereafter) followed that of protein expression (Fig. 1C). In the testis, both *E2f3a* and *E2f3ab* mRNA could be detected in Sertoli cells (Fig. 1C). In general, the *E2f3* mRNA signal was relatively weak throughout postnatal development, but the positive control probes yielded a strong signal especially in the adult testis (Fig. 1C, second and third rows). These data suggest that E2F3a expression is associated with Sertoli cell differentiation irrespective of the proliferation status of the Sertoli cells, while E2F3b is the primary isoform expressed in spermatogonia.

E2F3 is redundant in mouse Sertoli cells

To analyze the effect of *E2f3* loss on Sertoli cells, *Amh*-cre and $E2f3^{flox/flox}$ strains were crossbred (SC-$E2f3^{-/-}$). Surprisingly, *E2f3* appeared to be redundant in mouse Sertoli cells. The SC-$E2f3^{-/-}$ mice were viable and in good health at the ages of two and five months. The relative testis weights of the 2-month-old SC-$E2f3^{-/-}$ males were comparable to the controls, but at the age of five months there was a slight decrease in relative testis weight (Fig. S1A). The SC-$E2f3^{-/-}$ males sired healthy pups and there were no significant differences in the number of pups per litter as compared with the control males (Fig. S1B). Testicular histology appeared normal at both ages (Fig. S1C) and no changes were observed in the testicular cell populations on flow cytometric analysis (Fig. S1D). TUNEL-positive germ cells were quantified from seminiferous tubule cross-sections in stages VII–VIII to analyze germ cell apoptosis. The number of apoptotic cells was similar in control and SC-$E2f3^{-/-}$ seminiferous tubules (Fig. S1E). Sertoli cells express not only E2F3, but also E2F4 (El-Darwish et al., 2006) and there could be functional redundancy between these factors leaving *E2f3* dispensable for Sertoli cell development and function.

Knockout of *E2f3* in Sertoli cells rescues the spermatogenic failure associated with *Rb* loss

Loss of *Rb* in mouse Sertoli cells (SC-*Rb*KO) results in infertility due to Sertoli cell failure in adult life (Nalam et al., 2009; Rotgers et al., 2014). We have previously shown that shRNA-mediated knockdown of *E2f3 in vivo* leads to a partial rescue of the disruptive testicular phenotype of SC-*Rb*KO mice (Rotgers et al., 2014). Here, we cross-bred the SC-*Rb*KO (*Amh*-cre+; $Rb^{flox/flox}$) animals with $E2f3^{flox/flox}$ mice to study whether a complete loss of *E2f3* could fully rescue the SC-*Rb*KO phenotype. In $E2f3^{flox/flox}$ mice, exon 3 of the *E2f3* gene is flanked by loxP sites, and the sequence coding for the DNA-binding domain is excised by Cre recombinase and direct transcriptional control of gene expression by *E2f3* is abolished (Wu et al., 2001). In the *Amh*-cre mouse strain, constitutive expression of Cre begins on embryonic day (E)14.5 in Sertoli cells (Lécureuil et al., 2002).

The SC-$Rb^{-/-}E2f3^{+/+}$ (*Amh*-cre+; $Rb^{flox/flox}$; $E2f3^{wt/wt}$) animals had a similar testicular phenotype to the previously described SC-*Rb*KO mice (Fig. 2, Table 1) (Rotgers et al., 2014), despite a different hybrid genetic background. The primary time-point chosen for this study was the age of 2.5 months, because at this age the SC-*Rb*KO males showed a clear testicular phenotype, which allowed us to evaluate whether the loss of *E2f3* could rescue testicular defects (Rotgers et al., 2014).

The relative testis weight of *E2f3*-haploinsufficient (SC-$Rb^{-/-}E2f3^{+/-}$) and *E2f3*-knockout (SC-$Rb^{-/-}E2f3^{-/-}$) males were comparable to controls and significantly higher than in SC-$Rb^{-/-}E2f3^{+/+}$ males at the age of 2.5 months (Fig. 2A). The SC-$Rb^{-/-}E2f3^{+/+}$ males were infertile, while the added loss of *E2f3* resulted in rescue of the fertility, albeit not to a level comparable to the controls (Table 1).

Interestingly, loss of only one *E2f3* allele was not sufficient to fully overcome the effect of *Rb* loss. The SC-$Rb^{-/-}E2f3^{+/-}$ testes had some seminiferous tubules with a severe disruption of spermatogenesis (Fig. 2B, asterisks). The disruption became widespread and the testes resembled those of SC-$Rb^{-/-}E2f3^{+/+}$ males as the SC-$Rb^{-/-}E2f3^{+/-}$ males approached the age of 4 months (data not shown). The morphological changes associated with the SC-$Rb^{-/-}E2f3^{+/+}$ phenotype were similar to those previously shown and consisted of complete disruption of the seminiferous tubule architecture with massive germ cell loss and Leydig cell hyperplasia (Fig. 2B) (Nalam et al., 2009; Rotgers et al., 2014).

To assess whether the testicular phenotype had induced compensatory changes in the hypothalamic–pituitary axis, serum levels of luteinizing hormone (LH) and follicle-stimulating hormone (FSH) were measured in serum from 2.5-month-old animals. Despite the severe testicular phenotype in SC-$Rb^{-/-}E2f3^{+/+}$ males, no significant alterations were observed in either FSH or LH serum levels in the experimental groups as compared with controls. Androgen levels were analyzed from testicular homogenates using radio-immunoassay and testosterone content was normalized to the weight of the tissue (Table 1). Intra-testicular testosterone content was significantly higher in SC-$Rb^{-/-}E2f3^{+/+}$ testes as compared with SC-$Rb^{-/-}E2f3^{+/-}$ and a similar trend was observed when comparing

Journal of Cell Science (2019) 132, jcs229849. doi:10.1242/jcs.229849

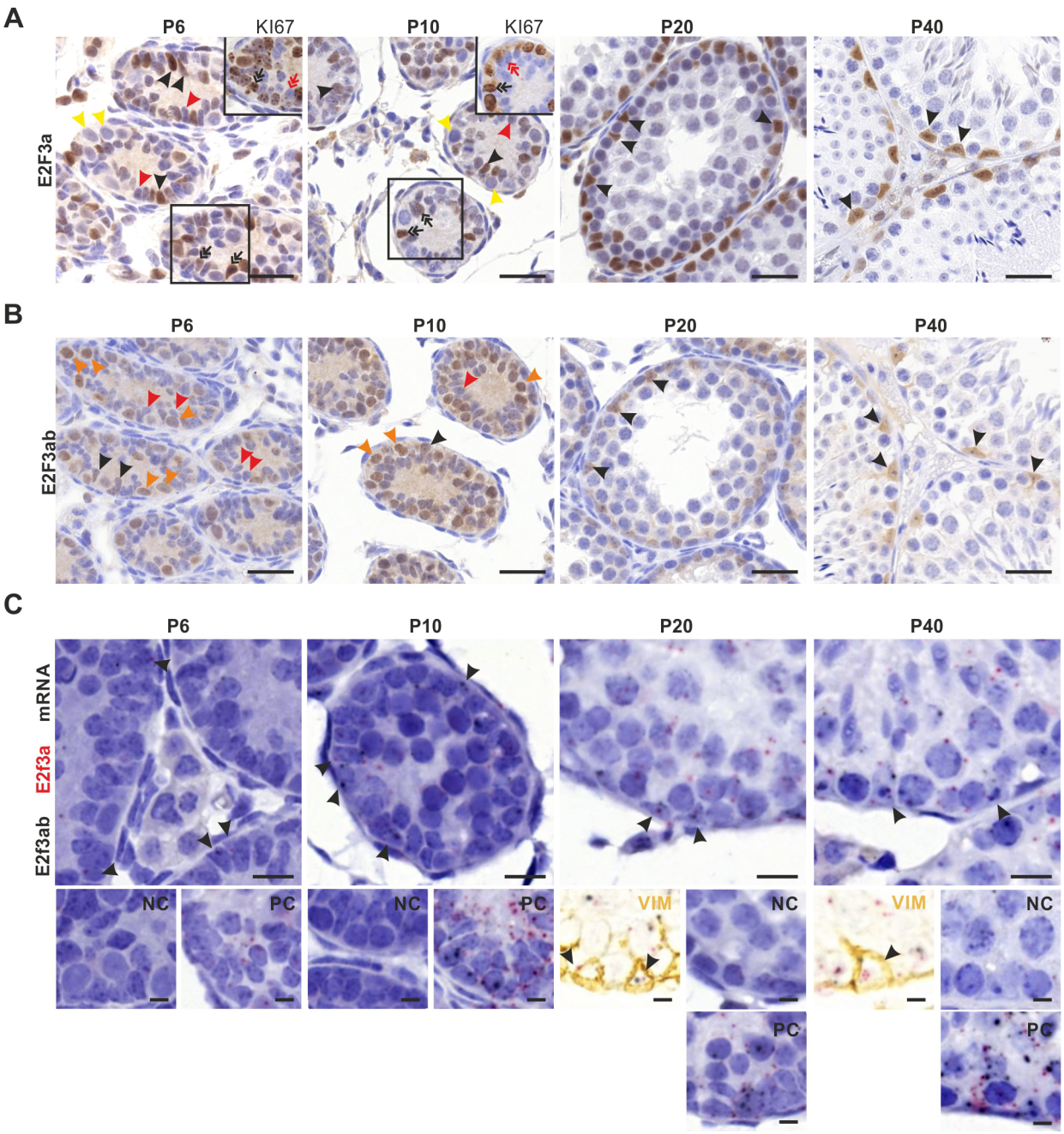

Fig. 1. E2F3a expression is induced in Sertoli cells upon differentiation. The expression pattern of E2F3a and E2F3ab was analyzed using RNA *in situ* hybridization and immunohistochemistry in postnatal mouse testis (ages P6, P10, P20 and P40). (A) E2F3a was expressed in a subpopulation of Sertoli cells at P6 [black arrowheads, E2F3a-positive (+) Sertoli cell; red arrowheads, E2F3a-negative (–) Sertoli cell] and the proportion of E2F3a+ Sertoli cells increased as the animals matured. By P20 all Sertoli cells showed a strong E2F3a signal. Germ cells were negative for E2F3a in all the time points studied (yellow arrowheads). Insets show proliferation marker KI67 on a consecutive section to identify the same Sertoli cells as in the E2F3a staining. Black double arrows, Sertoli cells stained for both E2F3a and KI67; red double arrows, E2F3a+ KI67– Sertoli cells. Both proliferative KI67+ and non-proliferative KI67– Sertoli cells expressed E2F3a. Scale bars: 25 µm (B) Antibody detecting both E2F3a and E2F3b isoforms (E2F3ab) showed positive staining in germ cells (orange arrowheads) and some Sertoli cells (black arrowheads, E2F3ab+; red arrowheads, E2F3ab–) on P6 and P10. Scale bars: 25 µm. (C) RNA *in situ* hybridization using probes specifically against mRNA encoding the *E2f3a* isoform, or a probe detecting both *E2f3a* and *E2f3b* isoforms (*E2f3ab*), showed mRNA expression in the same cell types where protein expression was detected. Immunohistochemical detection of vimentin was coupled to the RNA *in situ* hybridization to aid Sertoli cell identification in the P20 and P40 testes. Black, pan-E2F3; red, E2F3a; yellow, vimentin (VIM); blue, Mayer's hematoxylin. Arrowheads, E2F3a/E2F3ab-positive Sertoli cell. Lower panels show negative and positive controls for RNA in situ hybridization. PC, positive control probes (targeting common housekeeping gene); NC, negative control probes. Scale bars: 10 µm.

SC-$Rb^{-/-}E2f3^{+/+}$ to the control and SC-$Rb^{-/-}E2f3^{-/-}$ testes, although this was not significant because of high variation between individuals. Since there is excessive loss of germ cells in the SC-$Rb^{-/-}E2f3^{+/+}$ testis, the relative abundance of Leydig cells per mg of tissue is higher, which likely explains the increased testicular testosterone level when compared with control testes that have full spermatogenesis. However, we cannot exclude the possibility of Leydig cell hyperplasia resulting from impaired paracrine signaling in the testis.

Journal of Cell Science (2019) 132, jcs229849. doi:10.1242/jcs.229849

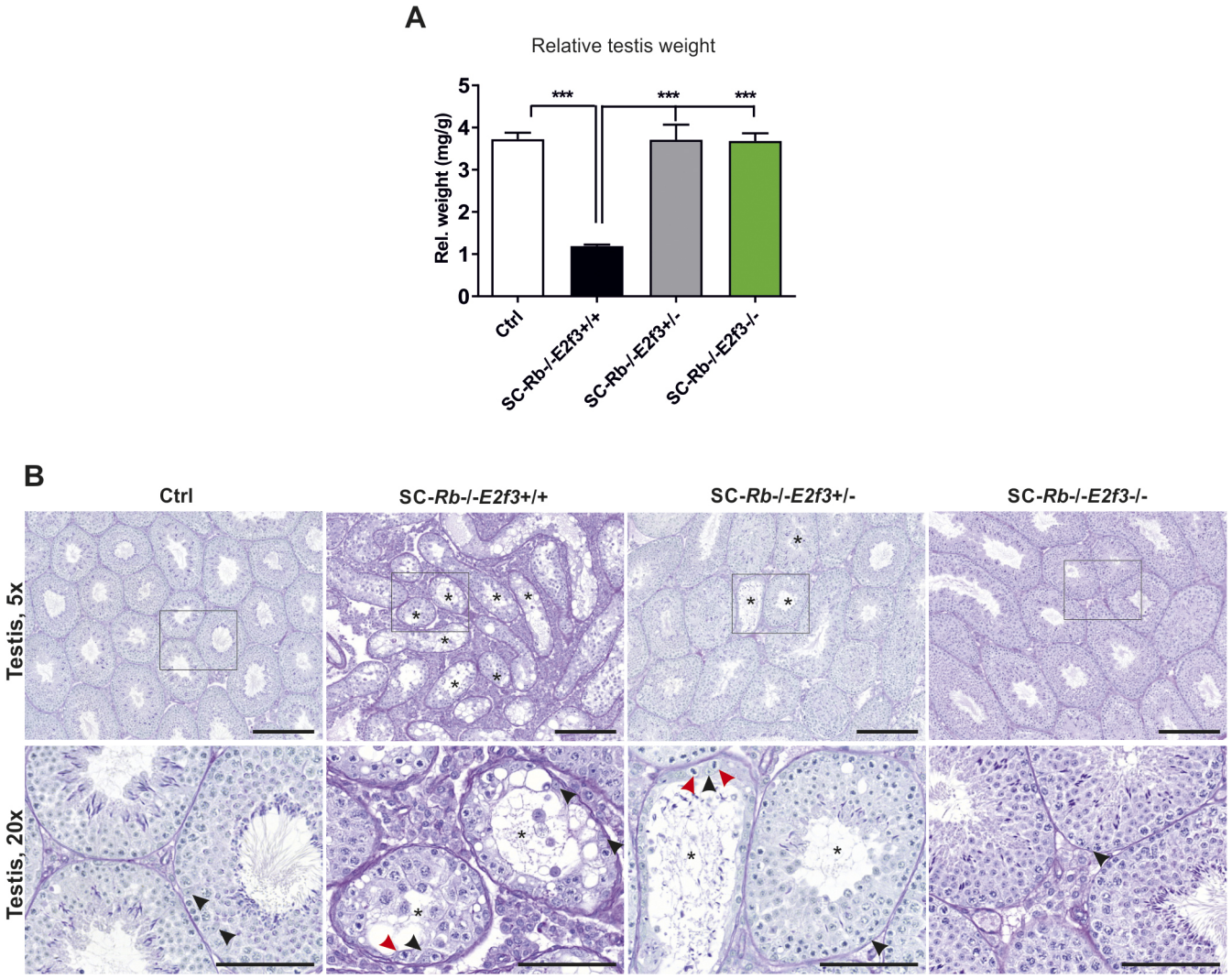

Fig. 2. Knockout of E2F3 in Sertoli cells rescues the failure of spermatogenesis caused by RB loss in Sertoli cells. (A) The reduced relative testis weight (testis weight/body weight) (mg/g) observed in SC-*Rb*$^{-/-}$*E2f3*$^{+/+}$ mice is restored to the same level as control in SC-*Rb*$^{-/-}$*E2f3*$^{+/-}$ and SC-*Rb*$^{-/-}$*E2f3*$^{-/-}$ mice. ***P<0.001. Statistical significance was calculated by one-way ANOVA followed by Tukey's test, n=8/group. Bars represent mean±s.e.m. (B) Representative PAS-stained testis histological sections. SC-*Rb*$^{-/-}$*E2f3*$^{+/+}$ testes are severely atrophied at the age of 2.5 months. The histology of the SC-*Rb*$^{-/-}$*E2f3*$^{-/-}$ testes is comparable to control, while SC-*Rb*$^{-/-}$*E2f3*$^{+/-}$ testes show focal seminiferous tubule atrophy. Squares in upper panels outline magnified area in lower panels. Asterisks, atrophied tubules; black arrowheads, Sertoli cells; red arrowheads, mitotic cell. Scale bar: 250 µm in upper panels, 100 µm in the lower panels.

E2F3 induced cell cycle re-entry in adult Sertoli cells in the absence of RB

Loss of *Rb* impairs cell cycle control in adult Sertoli cells and causes an increased Sertoli cell proliferation rate in adult SC-*Rb*KO testes (Nalam et al., 2009; Rotgers et al., 2014). Sertoli cell proliferation rate in adult testes was analyzed by quantifying KI67- and SOX9-positive Sertoli cells. As expected, loss of *Rb* resulted in a cell cycle re-entry of adult Sertoli cells, shown by an increased frequency of KI67-positive Sertoli cells in SC-*Rb*$^{-/-}$*E2f3*$^{+/+}$ testes (Fig. 3A,B). KI67-positive Sertoli cells were also observed in SC-*Rb*$^{-/-}$*E2f3*$^{+/-}$ testes, suggesting that even one copy of *E2f3a* was able to drive Sertoli cell cycle re-entry in the absence of *Rb*. In control testes, no proliferating Sertoli cells were detected (Fig. 3A,B). Lastly, no KI67-positive Sertoli cells were observed in the testes of 2.5-month-old SC-*Rb*$^{-/-}$*E2f3*$^{-/-}$ mice, showing that complete knockout of *E2f3* blocked ectopic Sertoli cell proliferation caused by *Rb* loss (Fig. 3A, B). In contrast to adult Sertoli cells, adult female supporting cells, granulosa cells, undergo active proliferation during folliculogenesis. However, proliferation of SC-*Rb*$^{-/-}$*E2f3*$^{+/+}$ Sertoli cells was not associated with Sertoli-to-granulosa cell transdifferentiation, as expression of the granulosa cell marker FOXL2 was not detected in SC-*Rb*$^{-/-}$*E2f3*$^{+/+}$ Sertoli cells (Fig. S2).

The cell cycle is tightly regulated, and different layers of cell cycle control can act redundantly when balance of the system is disrupted. In the *Rb*$^{-/-}$ fetal testis, loss of *Rb* is compensated by an induction of cyclin-dependent kinase inhibitor 1B (CDKN1B or p27^{Kip}) to achieve mitotic arrest of germ cells (Spiller et al., 2010). p27 can be inhibited by proteasomal degradation, and is targeted for proteasomal degradation by S-phase kinase-associated protein 2 (SKP2) (Carrano et al., 1999; Polyak et al., 1994). p27 did not show significant change in its expression, although it did tend to be higher in SC-*Rb*$^{-/-}$*E2f3*$^{+/+}$ testes (Fig. 3C). Interestingly, expression of p27-inhibiting *Skp2* was significantly downregulated in the SC-*Rb*$^{-/-}$*E2f3*$^{+/+}$ testes and normalized after *E2f3* deletion (Fig. 3D), suggesting that p27-dependent compensatory mechanisms operates not only in fetal germ cells, but also in adult

Journal of Cell Science (2019) 132, jcs229849. doi:10.1242/jcs.229849

Table 1. Characterization of the SC-*Rb*$^{-/-}$*E2f3*$^{-/-}$ and SC-*E2f3*$^{-/-}$ mouse line phenotypes

		2.5-month-old				2-month-old		5-month-old	
		Control	SC-*Rb*$^{-/-}$ *E2f3*$^{+/+}$	SC-*Rb*$^{-/-}$ *E2f3*$^{+/-}$	SC-*Rb*$^{-/-}$ *E2f3*$^{-/-}$	Control	SC-*E2f3*$^{-/-}$	Control	SC-*E2f3*$^{-/-}$
Body weight (g)	Mean	25.2	26.7	24.6	26.5	25.8	25.2	30.8	31.8
	s.e.m.	0.6	0.9	0.8	1.2	0.6	1.1	1.3	0.8
	95% CI	24–27	25–29	23–26	24–29	24–27	23–28	28–34	30–34
Relative testis weight (mg/g)	Mean	3.7	1.2***	3.7	3.7	3.8	4.0	3.6	3.1*
	s.e.m.	0.2	0.0	0.4	0.2	0.1	0.1	0.1	0.2
	95% CI	3.4–4.1	1.1–1.3	2.8–4.6	3.3–4.1	3.6–4.0	3.8–4.3	3.3–3.9	2.7–3.4
Epididymis weight (mg)	Mean	41	34*	40	43	40	40	55	52
	s.e.m.	2	1	2	2	1	2	2	1
	95% CI	36–46	32–36	35–45	39–47	36–43	35–45	50–60	49–55
Seminal vesicle weight (mg)	Mean	67	68*,[a]	55	73	58	60	96	87
	s.e.m.	2	6	5	4	4	6	7	7
	95% CI	62–72	55–81	44–66	64–81	48–68	46–74	79–112	69–105
Fertility test pups/litter	Mean	10	0***	6*	5**	6.083	6.415	3.833	1.918
	s.e.m.	0	0	1	1	1.788	0.5678	1.658	0.672
FSH (µg/l)	Mean	62	52	53	49	62	52	53.08	57.87
	s.e.m.	4	10	6	11	2	3	4.122	6.443
	95% CI	54–71	29–75	39–68	24–74	55–69	44–60	42–64	41–74
LH (µg/l)	Mean	0.4	0.4	1	1.4	2.5	3.2	1.7	1.4
	s.e.m.	0.1	0.1	0.4	0.5	0.6	1.2	0.7	0.4
	95% CI	0.1–0.7	0.1–0.7	0.2–1.9	0.2–2.7	1–3.8	0.3–6	−0.2–3.5	0.4–2.4
Intratesticular testosterone (ng/mg of tissue)	Mean	431.3	1267	234	325.3	448	123	n.a.	n.a.
	s.e.m.	330	458*,[a]	168	137	150	57		

One-way ANOVA followed by Tukey's post-test was used as a statistical test for the organ weight, fertility test, FSH and LH in the SC-*Rb*$^{-/-}$*E2f3*$^{-/-}$ study. Non-parametric Kruskal–Wallis test followed by Dunn's multiple comparison test was used to analyze the intratesticular testosterone assay in the SC-*Rb*$^{-/-}$ *E2f3*$^{-/-}$ study. Unpaired *t*-test was used to analyze the SC-*E2f3*$^{-/-}$ data at the two- and five-month time points. Statistical significance was analyzed compared to control, with the exception of values marked *,[a], which were compared with SC-*Rb*$^{-/-}$*E2f3*$^{+/-}$. ***P<0.001, **P<0.01, *P<0.05. n.a., not analyzed.

Sertoli cells to ensure cell cycle exit in the absence of *Rb*. Despite reactivated Sertoli cell proliferation (Fig. 3A,B), the expression level of Sertoli cell-associated transcripts (*Wt1*, *Sox9*, *Gata1*, *Gdnf*) remained unaffected (Fig. 3E), which is in agreement with the absence of expansion of the Sertoli cell population and tumor formation. The expression of markers of immature Sertoli cells (Amh and Thra) was not significantly increased in SC-*Rb*$^{-/-}$*E2f3*$^{+/+}$ testes, suggesting that, despite resuming proliferation, *Rb*-deficient Sertoli cells are capable of maintaining a transcriptional program typical of mature Sertoli cells (Fig. S3).

Loss of E2F3 improved the supportive capacity of RB-deficient Sertoli cells

Rb-deficient Sertoli cells failed to support spermatogenesis, which resulted in increased germ cell apoptosis shown in a TUNEL-assay (Fig. 4A,B) (Rotgers et al., 2014). The number of apoptotic germ cells (TUNEL-positive, SOX9-negative) was quantified from seminiferous epithelial stages VII–VIII to increase the sensitivity of detecting non-physiological germ cell apoptosis, because physiological germ cell apoptosis is absent in these stages. However, the epithelial stages could not be identified from SC-*Rb*$^{-/-}$*E2f3*$^{+/+}$ testes owing to germ cell loss, and thus random seminiferous tubule cross-sections were included in the analysis. When compared with the control, the SC-*Rb*$^{-/-}$*E2f3*$^{+/-}$ testes had more apoptotic germ cells in stages VII–VIII than the control (Fig. 4B), showing that the Sertoli cells were unable to support germ cell survival. However, the loss of both *E2f3* alleles in the SC-*Rb*$^{-/-}$*E2f3*$^{-/-}$ Sertoli cells resulted in a rescue of the supportive function of Sertoli cells, and germ cell apoptosis was comparable to the control testes (Fig. 4B).

To gain a quantitative insight into the changes in testicular cell population sizes, flow cytometry analysis was performed on enzymatically dissociated testicular tissue (Rotgers et al., 2015). As expected, based on the breakdown of spermatogenesis and infertility, the haploid cell population consisting of round and elongating spermatids was significantly smaller in the SC-*Rb*$^{-/-}$ *E2f3*$^{+/+}$ testes than in controls. Subsequently, this led to a relative overrepresentation of the diploid cell population, which included spermatogonia and somatic cells (Fig. 4C). SC-*Rb*$^{-/-}$*E2f3*$^{+/-}$ testes showed a slight decrease in the haploid cell population as compared with controls, while SC-*Rb*$^{-/-}$*E2f3*$^{-/-}$ testes did not differ from controls (Fig. 4C).

The expression of several pro- and anti-apoptotic genes was analyzed using targeted RNA sequencing. The relative expression of anti-apoptotic *Bcl-2* was significantly increased in SC-*Rb*$^{-/-}$ *E2f3*$^{-/-}$ testes in comparison with controls (Fig. 4D). By contrast, the level of apoptotic *Bax* was significantly increased in SC-*Rb*$^{-/-}$ *E2f3*$^{+/+}$, but not changed in SC-*Rb*$^{-/-}$*E2f3*$^{-/-}$ testes (Fig. 4D). Consequently, the *Bcl-2*:*Bax* ratio was increased in SC-*Rb*$^{-/-}$*E2f3*$^{-/-}$ testes (Fig. 4D), indicating activation of anti-apoptotic signaling. Pro-apoptotic *Trp53* expression was also decreased in SC-*Rb*$^{-/-}$*E2f3*$^{-/-}$ testes as compared with controls (Fig. 4D). Since the assay was performed on bulk RNA, it was not possible to distinguish gene expression changes between germ cells and Sertoli cells. However, altered *Bcl-2* levels can affect Sertoli cell biology. Transgenic overexpression of Bcl-2 in Sertoli cells results in a failure of spermatogenesis due to Sertoli cell dysfunction (Yamamoto et al., 2001). Increased Bcl-2 expression in SC-*Rb*$^{-/-}$*E2f3*$^{-/-}$ testes may reflect the activation of crucial anti-apoptotic machinery that contributes to the survival of Sertoli cells despite lacking *Rb*.

In addition, Sertoli cell dysfunction in SC-*Rb*$^{-/-}$*E2f3*$^{+/+}$ animals resulted in failure of the spermatogonial stem cell niche function, since relative expression levels of several spermatogonial stem cell markers [*Oct4* (also known as *Pou5f1*), *Lin28* (also known as *Lin28a*) and *Gfra1*] were significantly decreased in the SC-*Rb*$^{-/-}$ *E2f3*$^{+/+}$ testes as a sign of loss of this cell population, whereas in

Journal of Cell Science (2019) 132, jcs229849. doi:10.1242/jcs.229849

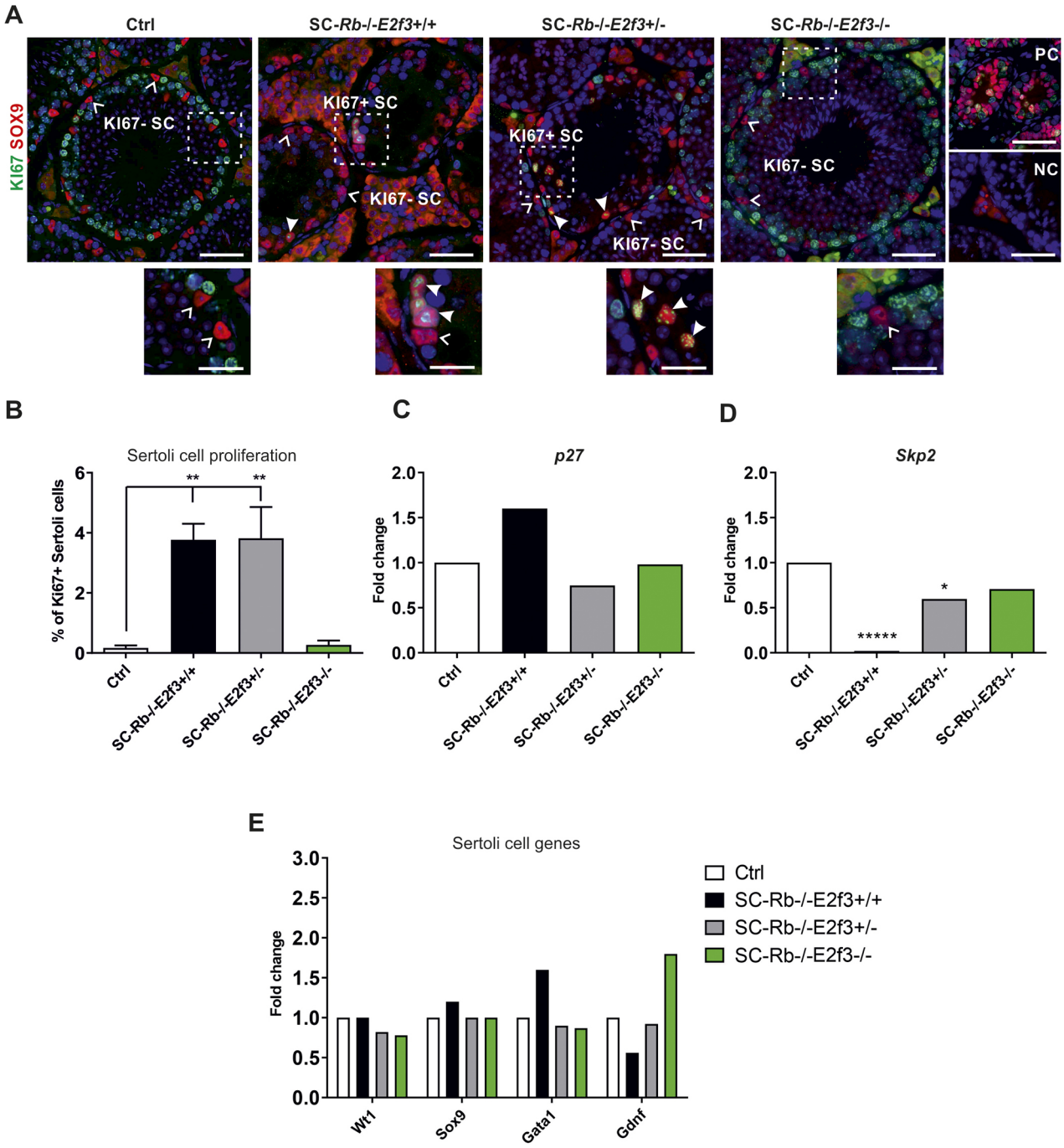

Fig. 3. E2F3 induced cell cycle re-entry in adult Sertoli cells in the absence of RB. (A) Sertoli cells (SOX9, red) and proliferating cells (KI67, green) were identified using immunofluorescence. There were no KI67-positive Sertoli cells (open arrowheads) in the control testes, but SC-$Rb^{-/-}E2f3^{+/+}$ and SC-$Rb^{-/-}E2f3^{+/-}$ testes had KI67-positive Sertoli cells (solid arrowheads). Knockout of E2F3 rescued the cell cycle re-entry. Squares in upper panels outline magnified area in lower panels. PC, positive control P6 mouse testis; NC, negative control. Scale bars: 50 µm and 25 µm in insets. (B) The number of KI67-positive Sertoli cells/100 Sertoli cells was quantified from four animals/group (three sections/animal). Bars represent mean±s.e.m. $^{**}P<0.01$. Statistical significance was calculated by one-way ANOVA followed by Tukey's test, n=3–4/group. (C) mRNA expression levels of the CDK inhibitor *p27* were not significantly changed in the experimental groups as compared with the controls. (D) In contrast with C, *Skp2*, which is an inhibitor of p27, showed significantly decreased expression in the SC-$Rb^{-/-}E2f3^{+/+}$ and SC-$Rb^{-/-}E2f3^{+/-}$ testes as compared with the controls. $^{*}P<0.05$, $^{*****}P<0.00001$. Statistical significance was calculated by negative binomial distribution model by the TruSeq Targeted RNA sequencing application v1.0, (n=4–5/group). (E) The mRNA levels of several Sertoli cell marker genes were quantified using targeted RNA sequencing. *Wt1*, *Sox9*, *Gata1* and *Gdnf* showed no significant changes between control and experimental groups.

SC-$Rb^{-/-}E2f3^{-/-}$ testes the levels were normal (Fig. 4E). Surprisingly, expression of markers for more differentiated spermatogonia [*Plzf* (also known as *Zbtb16*), *Stra8* and *Kit*] was not altered (Fig. 4E). The Leydig cell hyperplasia likely contributed to the high *Kit* mRNA level in SC-$Rb^{-/-}E2f3^{+/+}$ testes, since Kit is also expressed in Leydig cells (Manova et al., 1990). SC-$Rb^{-/-}E2f3^{+/+}$ testes also showed a significant decrease in meiotic cell markers (*Sycp1* and *Spo11*) and spermatid marker (*Piwil1*) mRNA, as expected based on the histological findings, and with *E2f3* deletion, these were normalized (Fig. 4E). These data indicate that

Journal of Cell Science (2019) 132, jcs229849. doi:10.1242/jcs.229849

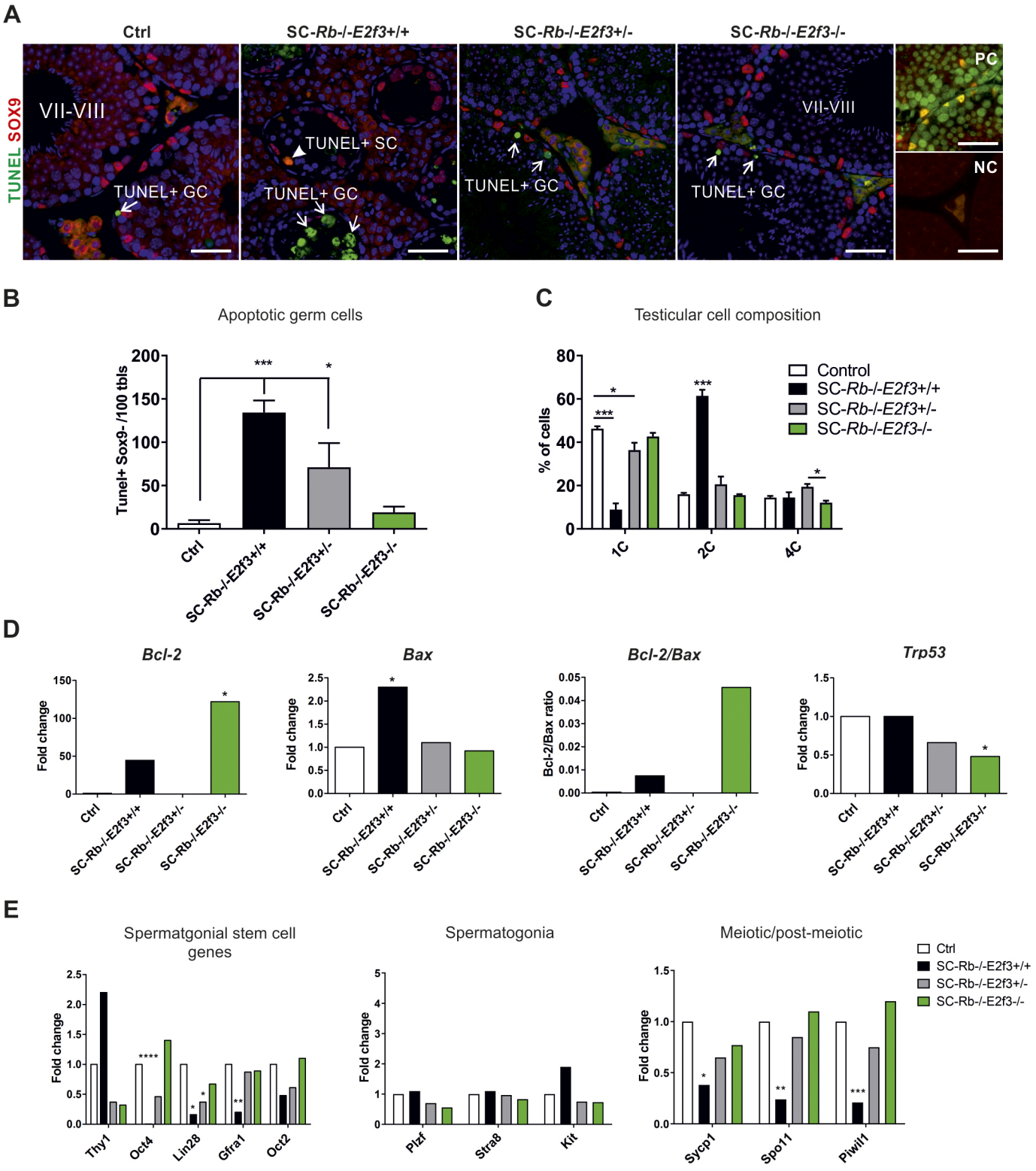

Fig. 4. See next page for legend.

RB is required in Sertoli cells to maintain their ability to support the spermatogonial stem cell niche, meiosis and haploid germ cell differentiation.

The loss of *Rb* in Sertoli cells led to a breakdown of Sertoli–germ cell junctions and sloughing of immature germ cells to the cauda epididymis (Fig. 5A, black arrows). This sloughing was rescued by additional loss of *E2f3*, since only spermatozoa were detected in the cauda epididymis of SC-$Rb^{-/-}E2f3^{-/-}$ epididymides (Fig. 5A).

Integrity of the seminiferous epithelium is maintained by the blood–testis barrier that forms between Sertoli cells and Sertoli–germ cell junctions such as the ectoplasmic specializations. Claudin 11 (CLDN11, blood–testis barrier) and espin (Espn, ectoplasmic

Journal of Cell Science (2019) 132, jcs229849. doi:10.1242/jcs.229849

Fig. 4. Loss of E2F3 in SC-*Rb*$^{-/-}$*E2f3*$^{+/+}$ testes rescues spermatogenesis. (A) Apoptotic cells and Sertoli cells were detected using the TUNEL assay (green) coupled to SOX9 (red). Apoptotic Sertoli cells were seen in the SC-*Rb*$^{-/-}$*E2f3*$^{+/+}$ testes while in the other groups the only apoptotic cells were the SOX9-negative germ cells. Arrowheads, TUNEL-positive (+) Sertoli cell (SC); arrows, TUNEL+ germ cell (GC); PC, positive control; NC, negative control. Scale bar: 50 µm. (B) Apoptotic germ cells (TUNEL+/SOX9−) were quantified from seminiferous tubule stages VII–VIII. In SC-*Rb*$^{-/-}$*E2f3*$^{+/+}$ testes random seminiferous tubule sections were selected for quantification, since seminiferous epithelial stages could not be classified. **P*<0.05, ****P*<0.001. Statistical significance was calculated by one-way ANOVA followed by Tukey's test, *n*=3–4/group. Bars represent mean±s.e.m. (C) Testicular cell composition was quantified using flow cytometry based on the DNA content of the cells (1C, haploid; 2C, diploid; 4C, tetraploid). The proportion of haploid cells in SC-*Rb*$^{-/-}$*E2f3*$^{-/-}$ testes was comparable to controls, but there was a slight decrease in the haploid cell population in SC-*Rb*$^{-/-}$*E2f3*$^{+/-}$ testes. ****P*<0.001, **P*<0.05. Statistical significance was calculated by one-way ANOVA followed by Tukey's test, *n*=5/group. Bars represent mean±s.e.m. (D) Targeted RNA sequencing was used to quantify several genes associated with apoptotic pathways. SC-*Rb*$^{-/-}$*E2f3*$^{-/-}$ testes showed a significant induction of the expression of the anti-apoptotic *Bcl-2*. SC-*Rb*$^{-/-}$*E2f3*$^{+/+}$ testes had increased expression of the apoptotic *Bax*. *Trp53* mRNA level was significantly decreased in SC-*Rb*$^{-/-}$*E2f3*$^{-/-}$ testes. (E) The expression of several marker genes for different germ cell populations was studied using targeted RNA sequencing. SC-*Rb*$^{-/-}$*E2f3*$^{+/+}$ testes showed a significant decrease in the expression of spermatogonial stem cell markers (*Oct4*, *Lin28* and *Gfra1*) and markers of meiotic (*Sycp1* and *Spo11*) and post-meiotic cells (*Piwil1*). (D,E) **P*<0.05, ***P*<0.01, ****P*<0.001, *****P*<0.0001. Statistical significance was calculated by negative binomial distribution model by the TruSeq Targeted RNA sequencing application v1.0, (*n*=4–5/group).

specializations) showed a disrupted expression pattern in all the seminiferous tubules of SC-*Rb*$^{-/-}$*E2f3*$^{+/+}$ testes (Fig. 5B, asterisk), while the majority of the seminiferous tubules in SC-*Rb*$^{-/-}$*E2f3*$^{+/-}$ testes were intact, and in SC-*Rb*$^{-/-}$*E2f3*$^{-/-}$ testes no disruption was observed (Fig. 5B). Relative expression of *Cldn11* was not significantly altered by loss of *Rb* in Sertoli cells (Fig. 5C).

Claudin 3 (CLDN3) localizes to newly formed tight junctions between Sertoli cells in seminiferous epithelial stages VIII–X (Meng et al., 2005; Smith and Braun, 2012). Moreover, *Cldn3* expression has been shown to be co-activated by RB and androgen receptor (AR) in Sertoli cells *in vitro* (Wu et al., 2013) and loss of *Ar in vivo* results in a loss of *Cldn3* expression (Meng et al., 2005). Correspondingly, SC-*Rb*$^{-/-}$*E2f3*$^{+/+}$ testes showed significantly decreased expression of *Cldn3* mRNA, while the additional loss of *E2F3* in Sertoli cells restored *Cldn3* expression to close to normal (Fig. 5E). This suggests that *Rb* is involved in controlling *Cldn3* expression in Sertoli cells *in vivo* and that this control is mediated by transcription factor E2F3.

We hypothesized that the focal disruption of the seminiferous epithelium in SC-*Rb*$^{-/-}$*E2f3*$^{+/-}$ testes (Fig. 2B) was associated with a defect of Sertoli cell cycling during the seminiferous epithelial cycle. The stage-specific cycling behavior of Sertoli cells was analyzed by using AR expression pattern as a proxy, since AR staining intensity fluctuates depending on the seminiferous epithelial stage (Bremner et al., 1994). The stage-specificity of AR expression was retained in Sertoli cells in all experimental groups, with a strong AR signal in Sertoli cell nuclei in seminiferous epithelial stages V–VI and a low signal in stages X–XI (Fig. 5F). Even in SC-*Rb*$^{-/-}$*E2f3*$^{+/+}$ testes, where discerning the seminiferous epithelial stages based on germ cell morphology was not possible, a clear fluctuation of AR intensity between tubule cross sections could be observed (Fig. 5F, tubules marked with H for high expression and L for low expression). Furthermore, relative *Ar* expression showed no changes when compared to control (Fig. 5D). These results indicate that the RB–E2F3 pathway does not control AR expression in Sertoli cells.

Loss of *E2f3* restores transcriptional defects caused by loss of *Rb*

In the absence of *Rb*, other RB family proteins p107 (also known as Rbl1) and p130 (also known as Rbl2) achieve a level of compensation for RB by binding to E2F3 in Sertoli cells (Rotgers et al., 2014). To facilitate this compensation, ectopic expression of p107 is triggered in Sertoli cells on *Rb* loss (Rotgers et al., 2014). The expression patterns of p107 and p130 were analyzed in testes of *Rb* and *E2f3* double-knockout animals (SC-*Rb*$^{-/-}$*E2f3*$^{-/-}$). Immunohistochemistry revealed that ectopic expression of p107 in Sertoli cells after loss of *Rb* was abolished by simultaneous knockout of *E2f3* (SC-*Rb*$^{-/-}$*E2f3*$^{-/-}$) (Fig. 6A). By contrast, *p107* mRNA levels were decreased in SC-*Rb*$^{-/-}$*E2f3*$^{+/+}$ testes but this likely reflected the loss of the pachytene spermatocytes that express p107, rather than a transcriptional change in Sertoli cells (Fig. 6C). In wild-type testes, p130 is expressed in Sertoli cells, and this expression pattern was unaltered in SC-*Rb*$^{-/-}$*E2f3*$^{+/+}$, SC-*Rb*$^{-/-}$*E2f3*$^{+/-}$ and SC-*Rb*$^{-/-}$*E2f3*$^{-/-}$ testes (Fig. 6B), but a strong downregulation of *p130* mRNA was observed in SC-*Rb*$^{-/-}$*E2f3*$^{+/+}$ testes (Fig. 6C). As expected, *Rb* mRNA levels were downregulated in the testes of SC-*Rb*$^{-/-}$*E2f3*$^{+/+}$, SC-*Rb*$^{-/-}$*E2f3*$^{+/-}$ and SC-*Rb*$^{-/-}$*E2f3*$^{-/-}$ animals (Fig. 6C). *Rb* is also expressed in spermatogonia, which are not targeted by *Amh*-cre, which explains the residual *Rb* expression in knockout testes.

Loss of *E2f3* in Sertoli cells did not result in compensatory transcriptional induction of transcriptional activator *E2f1* (Fig. 6D). However, expression of transcriptional repressors E2F4 and E2F5 was decreased in SC-*Rb*$^{-/-}$*E2f3*$^{+/+}$ testes (Fig. 6D). E2F4 is expressed in mouse Sertoli cells and could be subject to negative regulation by *E2f3* (El-Darwish et al., 2006). In contrast, the decrease in *E2f5* expression likely reflected the loss of preleptotene spermatocytes in SC-*Rb*$^{-/-}$*E2f3*$^{+/+}$ testes, since it is not expressed in Sertoli cells in mouse testes (Fig. 6D) (El-Darwish et al., 2006). Similarly, the decrease in cyclin B1 (*Ccnb1*) and cyclin E2 (*Ccne2*) expression in SC-*Rb*$^{-/-}$*E2f3*$^{+/+}$ testes (Fig. 6E) likely reflected a loss of late pachytene spermatocytes (Gromoll et al., 1997; Martinerie et al., 2014). Cyclin E1 (*Ccne1*), which is expressed in Sertoli cells (Martinerie et al., 2014), did not show altered expression in comparison with controls (Fig. 6E), suggesting that deregulated *E2f3* activity did not drive Sertoli cells to proliferate by transcriptionally upregulating cyclin E.

Since E2F3 is a transcription factor, we were interested in analyzing the effect of *E2f3* loss on the expression of putative E2F target genes in the testis to find possible downstream effectors of *E2f3*. The putative E2F target genes were chosen both directly from literature (Bracken et al., 2004) and through cross-comparisons of experimental data. The lists of differentially expressed genes in earlier SC-*Rb*KO studies (Nalam et al., 2009; Rotgers et al., 2014) were compared to ChIP-on-CHIP datasets, where binding of E2F1 and E2F3 to promoters was studied in mouse cells (Asp et al., 2009; Cao et al., 2011). As expected, based on the experimental design, control and SC-*Rb*$^{-/-}$*E2f3*$^{+/+}$ testes showed differential expression of many of these genes as shown in the heatmap (Fig. 6F). SC-*Rb*$^{-/-}$*E2f3*$^{+/-}$ and SC-*Rb*$^{-/-}$*E2f3*$^{-/-}$ more closely resembled expression patterns in control testes than SC-*Rb*$^{-/-}$*E2f3*$^{+/+}$ testes (Fig. 6F).

Follistatin expression was regulated in an RB–E2F3-dependent manner in the mouse testis

Follistatin (*Fst*) is a putative E2F3 target gene (Müller et al., 2001) and it is a key player in paracrine and endocrine control of testis by the TGFβ superfamily (for a recent review see Wijayarathna and de Kretser, 2016). *Fst* expression was strongly induced in SC-*Rb*$^{-/-}$

Journal of Cell Science (2019) 132, jcs229849. doi:10.1242/jcs.229849

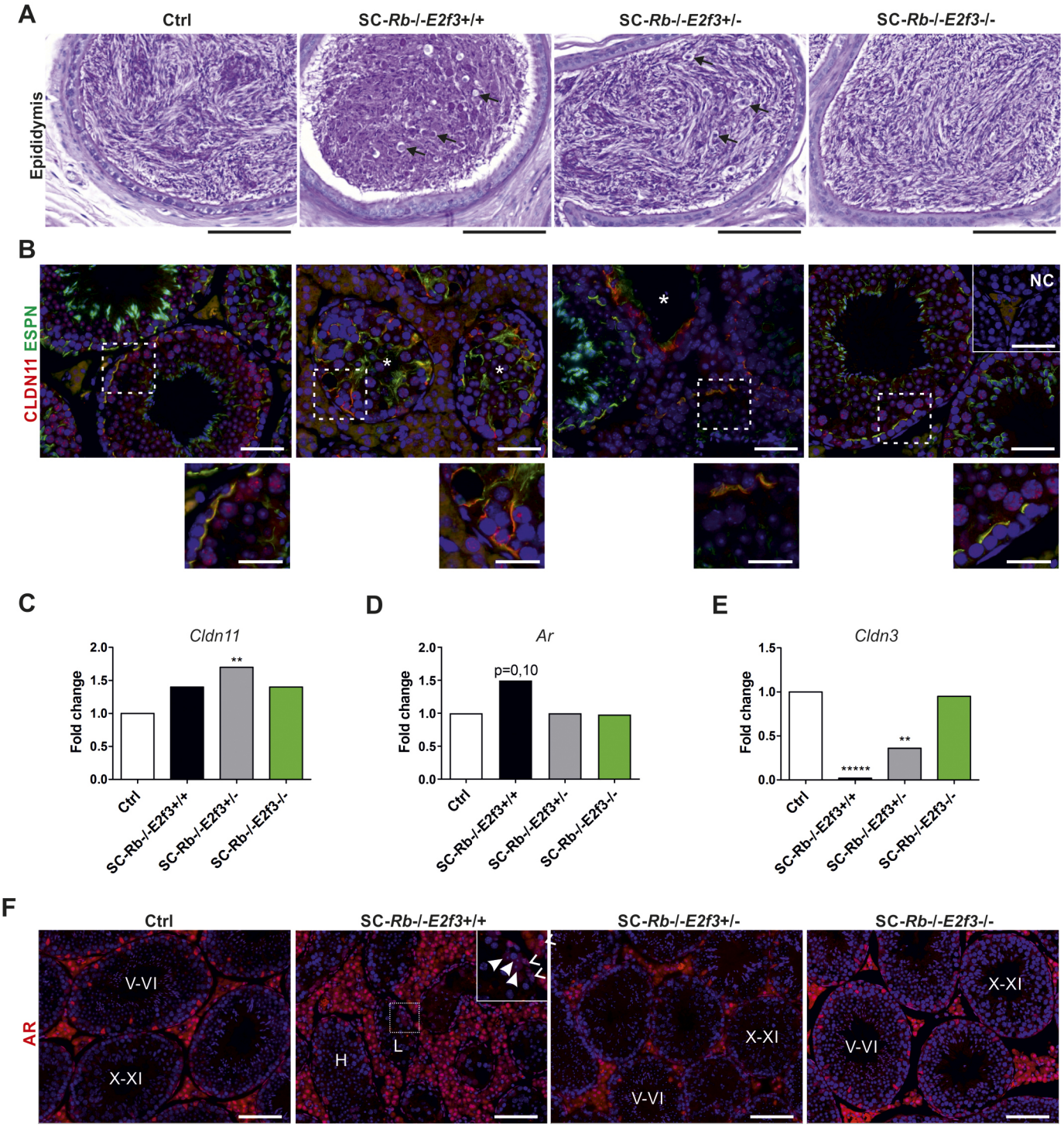

Fig. 5. Loss of germ cells was associated with a disruption of Sertoli cell tight junctions and ectoplasmic specialization. (A) Immature germ cells detach from Sertoli cell prematurely in SC-*Rb*$^{-/-}$*E2f3*$^{+/+}$ and SC-*Rb*$^{-/-}$*E2f3*$^{+/-}$ testes and travel to the cauda epididymis. Arrows, immature germ cells. Scale bars: 100 µm. (B) Sertoli–Sertoli junctions at the blood–testis barrier (Claudin11, red) and ectoplasmic specializations (Espin, green) were disrupted in SC-*Rb*$^{-/-}$*E2f3*$^{+/+}$ and SC-*Rb*$^{-/-}$*E2f3*$^{+/-}$ seminiferous tubules with germ cell loss (asterisk), but intact throughout the testes in control and SC-*Rb*$^{-/-}$*E2f3*$^{-/-}$ animals. Scale bars: 50 µm and 25 µm in insets. (C) *Cldn11* mRNA expression was slightly elevated in SC-*Rb*$^{-/-}$*E2f3*$^{+/-}$ testes in comparison with control. (D) *Ar* expression was not significantly altered in any of the experimental groups. (E) Claudin3 (*Cldn3*) associates with the newly developing tight-junctions during preleptotene spermatocyte transition to the lumen. In the SC-*Rb*$^{-/-}$*E2f3*$^{+/+}$ and SC-*Rb*$^{-/-}$*E2f3*$^{+/-}$ *Cldn3* mRNA was significantly down-regulated in comparison with the control. (C–E) ***P*<0.01, ******P*<0.0001. Statistical significance was calculated by negative binomial distribution model by the TruSeq Targeted RNA sequencing application v1.0, (*n*=4–5/group). (F) Sertoli cells showed a stage-specific fluctuation in androgen receptor (AR) expression in all the experimental groups with high AR levels in seminiferous epithelial stages V–VI and low levels in stages X–XI. In SC-*Rb*$^{-/-}$*E2f3*$^{+/+}$ testes there were seminiferous tubules with a high (H) and low (L) AR expression, but identifying the stages was not possible. Inset shows magnification of the area marked by a white square. Open arrowhead, AR-positive peritubular myoid cell; solid arrowhead, Sertoli cell with a low AR expression. Scale bars: 50 µm.

Journal of Cell Science (2019) 132, jcs229849. doi:10.1242/jcs.229849

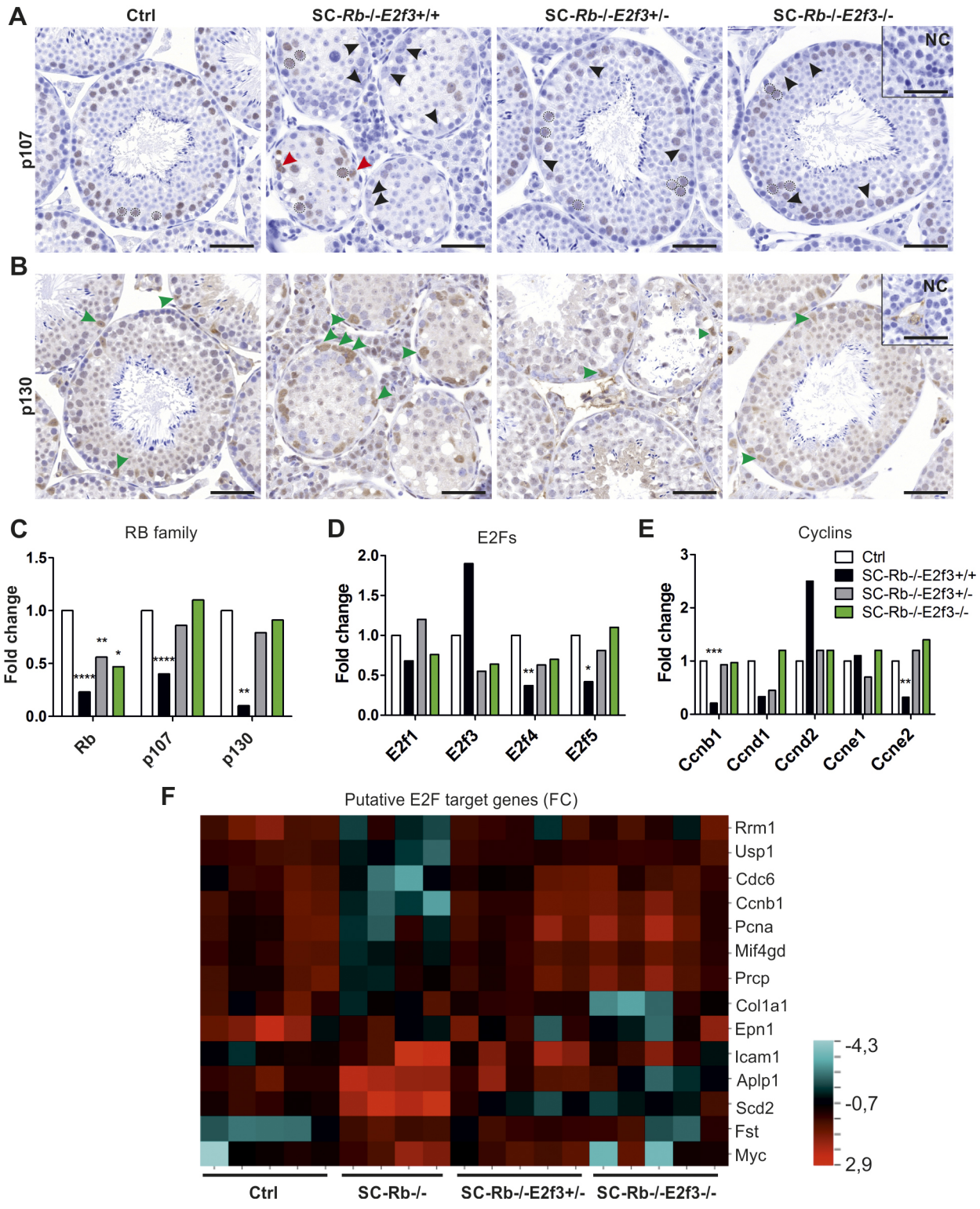

Fig. 6. See next page for legend.

$E2f3^{+/+}$ testes and decreased after ablation of *E2f3* in a dose-dependent manner (Fig. 7A). Follistatin inhibits activin by direct binding (Nakamura et al., 1990). Activin forms as homo- and heterodimers of inhibin beta subunits, which are encoded by the *inhibin beta A* (*Inhba*) and *inhibin beta B* (*Inhbb*) genes (Ling et al., 1986). The expression of *Inhba* and *Inhbb* transcripts was not altered in SC-$Rb^{-/-}E2f3^{+/+}$ testes compared to controls (Fig. 7B–D). When inhibin beta subunits dimerize with inhibin alpha (Inha) subunits they form inhibin A and inhibin B (Robertson et al., 1985). Knockout of the Inha subunit in mice leads to an increase in activin A production, which results in formation of Sertoli–granulosa cell tumors and cachexia (Matzuk et al., 1992). Nevertheless, *Inha* expression was not altered in SC-$Rb^{-/-}E2f3^{+/+}$ testes (Fig. 7B). Transcription factor SMAD4 is a central downstream effector of

Journal of Cell Science

Journal of Cell Science (2019) 132, jcs229849. doi:10.1242/jcs.229849

Fig. 6. RB family proteins, E2Fs and cyclins in Sertoli cell-cycle control. (A,B) RB family proteins p107 and p130 were expressed in a similar manner in control, SC-*Rb*$^{-/-}$*E2f3*$^{+/-}$ and SC-*Rb*$^{-/-}$*E2f3*$^{-/-}$ testes. (A) Ectopic p107 expression was detected in SC-*Rb*$^{-/-}$*E2f3*$^{+/+}$ Sertoli cells (red arrowheads) as previously described (Rotgers et al., 2014). Dashed circles outline pachytene spermatocytes. Black arrowheads, p107-negative Sertoli cells; red arrowheads, p107-positive Sertoli cells; NC, negative control. Scale bars: 50 µm. (B) p130 immunohistochemistry. Green arrowheads, p130-positive Sertoli cell. Scale bars: 50 µm. (C–E) Quantification (as fold change) of cell cycle-related genes of the RB family (C), E2Fs (D) and cyclins (E). (C) *p107* and *p130* were downregulated in SC-*Rb*$^{-/-}$*E2f3*$^{+/+}$ testes. (E) The decrease in *Ccnb1* and *Ccne2* mRNA levels likely reflected the loss of spermatocytes. Experimental groups were compared to controls using the TruSeq Targeted RNA sequencing application and the *P*-value represents the significance of the comparison of the group to control. **P*<0.05, ***P*<0.01, ****P*<0.001, *****P*<0.0001. (F) A heatmap depicting the fold-change (FC) of expression of the selected putative E2F target genes in mouse testis. Only genes with a significantly altered expression in pairwise comparisons of the normalized read counts were selected for the heatmap. Control and SC-*Rb*$^{-/-}$*E2f3*$^{+/+}$ testes showed differential expression of several of the genes, while SC-*Rb*$^{-/-}$*E2f3*$^{+/-}$ and SC-*Rb*$^{-/-}$*E2f3*$^{-/-}$ testes mostly resembled controls. Statistical significance was calculated by negative binomial distribution model by the TruSeq Targeted RNA sequencing application v1.0, (*n*=4–5/group).

TGFβ family signaling (Wijayarathna and de Kretser, 2016). *Smad4* expression was significantly decreased in SC-*Rb*$^{-/-}$*E2f3*$^{+/-}$ and SC-*Rb*$^{-/-}$*E2f3*$^{-/-}$ testes compared to control (Fig. 7E), suggesting that the increase in *Fst* expression could lead to suppression of TGFβ family signaling. Taken together, these data suggest that *Fst* expression is increased in the absence of *Rb* by a potentially E2F3-dependent mechanism, independently of other TGFβ family members.

DISCUSSION

Rb controls the maintenance of Sertoli cell quiescence and terminal differentiation in adulthood (Nalam et al., 2009; Rotgers et al., 2014). We have previously shown that RB interacts with E2F3 during testicular development, and that shRNA-mediated knockdown of *E2f3* alleviated the degenerative phenotype associated with loss of *Rb* in Sertoli cells (Rotgers et al., 2014). In this study, we used *E2f3*$^{flox/flox}$ mice to achieve a complete knockout of *E2f3* in Sertoli cells and to obtain a more robust model for *E2f3* knockdown than *in vivo* shRNA for studying the role of the RB–E2F3 pathway in mouse Sertoli cells.

Sertoli cell dysfunction in SC-*Rb*$^{-/-}$*E2f3*$^{+/+}$ testes was identical to that previously published (Rotgers et al., 2014) and these animals showed a disruption of spermatogenesis due to a combined failure of the spermatogonial stem cell niche, increased germ cell apoptosis and breakdown of Sertoli–germ cell junctions. Sertoli cell dysfunction was rescued by loss of *E2f3*. SC-*Rb*$^{-/-}$*E2f3*$^{+/-}$ testes showed a complete rescue of spermatogenesis in the majority of seminiferous tubules on a morphological level when compared with SC-*Rb*$^{-/-}$*E2f3*$^{+/+}$ testes in 2.5-month-old animals. However, by the age of four months, SC-*Rb*$^{-/-}$*E2f3*$^{+/-}$ animals, with one remaining functional *E2f3* allele, showed a similar level of testis disruption as SC-*Rb*$^{-/-}$*E2f3*$^{+/+}$ animals (data not shown). In addition, SC-*Rb*$^{-/-}$*E2f3*$^{+/-}$ testes showed Sertoli cell proliferation at a similar rate as in SC-*Rb*$^{-/-}$*E2f3*$^{+/+}$ testes in the 2.5-month-old mice, suggesting that a single copy of *E2f3* is sufficient to drive adult Sertoli cell proliferation in the absence of *Rb*, and this ultimately leads to a complete disruption of spermatogenesis. However, a complete loss of *E2f3* in Sertoli cells of SC-*Rb*$^{-/-}$*E2f3*$^{-/-}$ mice led to a sustained rescue of spermatogenesis and Sertoli cell quiescence status. Moreover, when Rbf (*Drosophila* homolog of RB) is knocked down in hub cells, which are the somatic component of the stem cell niche in the *Drosophila* testis, the hub cells exit the quiescent state and form ectopic stem cells niches. Similarly to our model, ectopic hub cell proliferation is rescued by a simultaneous knockdown of E2F, indicating a conserved role of an RB–E2F switch in the control of testicular nurse cell quiescence (Greenspan and Matunis, 2018). E2Fs also drive cell proliferation in the absence of RB in several other cell types; loss of *E2f3* can rescue defects in proliferation and apoptosis in *Rb*-deficient lens and CNS cells (Ziebold et al., 2001) and pituitary tumors in *Rb*$^{-/-}$ mice can be rescued by *E2f3* deletion (Ziebold et al., 2003). In conclusion, RB-mediated inhibition of E2F3 is essential for the maintenance of quiescence in adult Sertoli cells, which is in agreement with the role of E2F3 as a driver of cell cycle progression.

The *E2f3* locus encodes two isoforms, E2F3a and E2F3b, through the use of alternative promoters, and these can have opposing roles in regulating cell fate (Danielian et al., 2008). E2F3a expression was gradually induced in mouse Sertoli cells upon postnatal maturation. RB and E2F3 interact in mouse Sertoli cells on P10, which coincides with the induction of the cell cycle exit period as Sertoli cells mature in puberty (Rotgers et al., 2014; Zimmermann et al., 2015). It is possible that transcription factor E2F3a recruits RB to the promoters of genes associated with Sertoli cell proliferation to induce gene silencing, and/or to genes associated with maturation, to activate transcription. We hypothesized that acquiring E2F3a expression in Sertoli cells was associated with cell cycle exit during maturation. However, expression of proliferation marker KI67 and E2F3a did not correlate in the juvenile testis as some E2F3a-positive Sertoli cells were positive for KI67 while others were negative. Furthermore, *E2f3* is dispensable for cell cycle progression of mouse Sertoli cells, since loss of *E2f3* did not affect testis size in SC-*E2f3*$^{-/-}$ mice, indicating that Sertoli cell proliferation was not compromised during development. This could result from compensation for *E2f3* loss by the other E2Fs, since the activator E2Fs show extensive redundancy during development (Kong et al., 2007). Only E2F3 and the repressive E2F4 are expressed in wild-type mouse Sertoli cells (El-Darwish et al., 2006) and SC-*Rb*$^{-/-}$*E2f3*$^{+/+}$ testes showed a decreased expression of *E2f4*, rather than an increase. However, we cannot exclude the possibility that E2F4 compensates for E2F3 in transcriptional control of Sertoli cells since RB can interact with both E2F3 and E2F4, and the E2Fs share a similar consensus DNA-binding site (Moberg et al., 1996; Zheng et al., 1999).

One of the E2F target genes that showed a high level of induction in SC-*Rb*$^{-/-}$*E2f3*$^{+/+}$ testes was *Fst* (Müller et al., 2001). *Fst* is highly expressed in immature mouse testes and its expression gradually decreases as the animals mature (Barakat et al., 2008). Interestingly, transgenic expression of *Fst* in the testis results in a phenotype very similar to that of SC-*Rb*$^{-/-}$*E2f3*$^{+/+}$ and SC-*Rb*$^{-/-}$*E2f3*$^{+/-}$ testes (Guo et al., 1998). In particular, *Fst* transgenic testes exhibit a similar focal seminiferous tubule disruption as observed in SC-*Rb*$^{-/-}$*E2f3*$^{+/-}$ testes (Guo et al., 1998). *Fst* expression was dependent on the E2F3 status of Sertoli cells, with expression significantly increased in SC-*Rb*$^{-/-}$*E2f3*$^{+/+}$ testes and decreased in response to the loss of *E2f3*, in a dose-dependent manner. We hypothesize that RB and E2F3 act as a complex to repress *Fst* expression in adult wild-type Sertoli cells. By contrast, E2F3 induces *Fst* expression in the absence of RB in SC-*Rb*$^{-/-}$*E2f3*$^{+/+}$ testes, and increased *Fst* expression could contribute to the loss of Sertoli cell function. Alternatively, rather than being a driver of the phenotype, increased *Fst* expression could merely be a consequence of reactivated Sertoli cell proliferation in adulthood, as FST inhibits activin A, which promotes Sertoli cell proliferation (Archambeault and Yao, 2014).

The maintenance of quiescence in Sertoli cells is closely connected to the maintenance of the blood–testis barrier. Loss of

Journal of Cell Science (2019) 132, jcs229849. doi:10.1242/jcs.229849

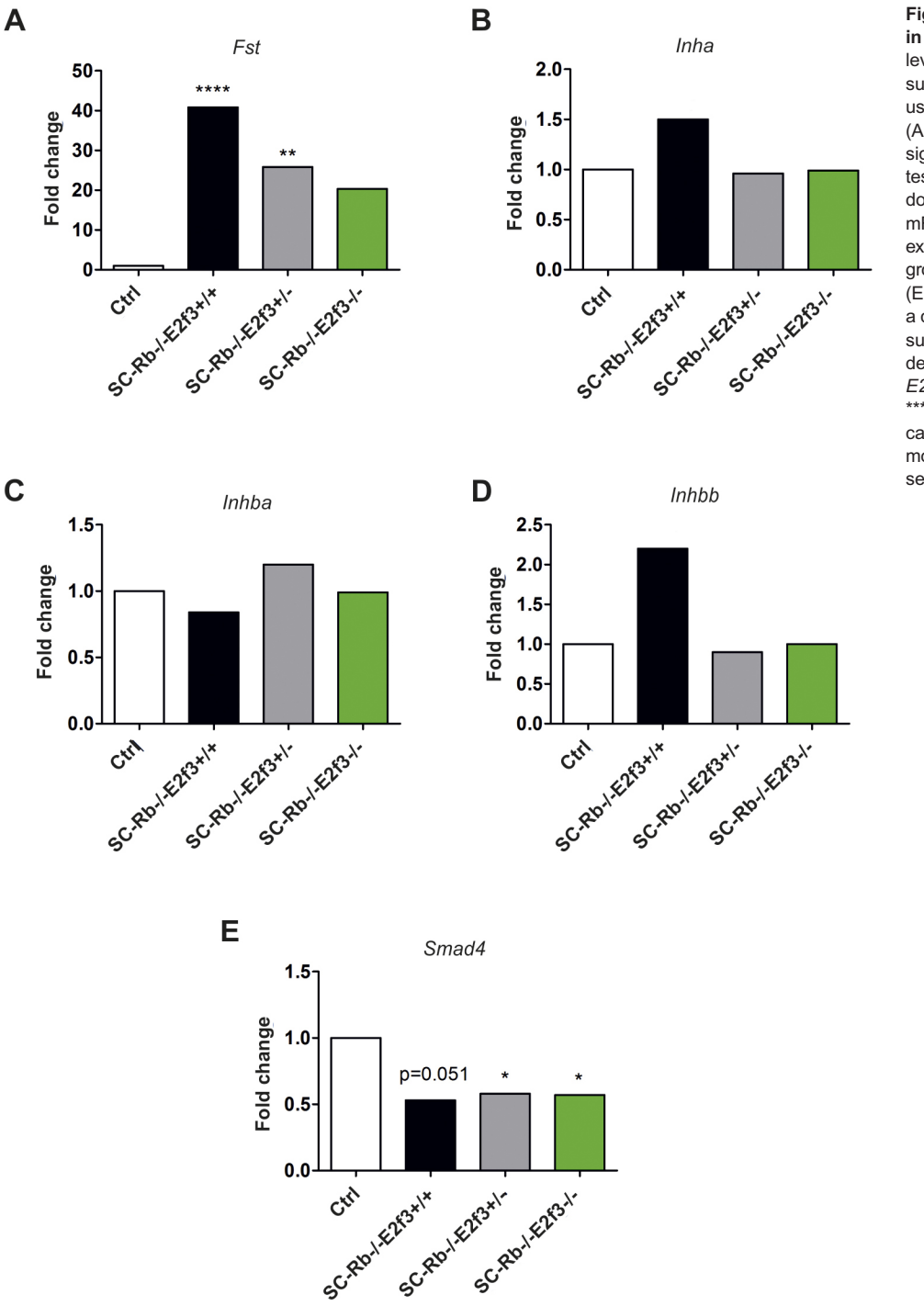

Fig. 7. Follistatin expression is increased in SC-*Rb*$^{-/-}$*E2f3*$^{+/+}$ testes. The mRNA levels of several components of the TGFβ superfamily signaling pathway were studied using targeted RNA sequencing. (A) Follistatin (*Fst*) expression was significantly increased in SC-*Rb*$^{-/-}$*E2f3*$^{+/+}$ testes. Loss of E2F3 was associated with a dose-dependent decrease in testicular *Fst* mRNA levels. (B–D) *Inha*, *Inhba* and *Inhbb* expression was unaltered in the experimental groups in comparison with the controls. (E) Expression of transcription factor *Smad4*, a common downstream effector of TGFβ superfamily signaling, was significantly decreased in SC-*Rb*$^{-/-}$*E2f3*$^{+/-}$ and SC-*Rb*$^{-/-}$*E2f3*$^{-/-}$ testes. *P<0.05, **P<0.01, ****P<0.0001. Statistical significance was calculated by negative binomial distribution model by the TruSeq Targeted RNA sequencing application v1.0, (n=4–5/group).

Cldn11, an integral part of tight junctions on the blood–testis barrier, results in both failure of supporting spermatogenesis and reactivation of Sertoli cell proliferation in the adult, but no apparent dedifferentiation (Gow et al., 1999; Mazaud-Guittot et al., 2010). Knockout of gap junction protein connexin-43 (CX43, also known as GJA1) leads to a similar phenotype with continued Sertoli cell proliferation in adulthood, sloughing of Sertoli cells to seminiferous tubule lumen and a failure of spermatogenesis (Sridharan et al., 2007). In our study, *Rb* appeared to have a direct role in controlling the expression of Cldn3, a tight junction protein associated with the newly formed blood–testis barrier (Smith and Braun, 2012), since *Cldn3* mRNA levels were dramatically decreased in SC-*Rb*$^{-/-}$*E2f3*$^{+/+}$ testes. It has been shown *in vitro* that RB and AR co-activate *Cldn3* expression in Sertoli cells (Wu et al., 2013) and that a loss of *Ar* in Sertoli cells decreases *Cldn3* expression and increases the permeability of the blood–testis barrier (De Gendt et al., 2004; Meng et al., 2005). The loss of *E2f3* in SC-*Rb*$^{-/-}$*E2f3*$^{-/-}$ testes restored expression of *Cldn3* to a normal level. Our results suggest that *Rb* controls *Cldn3* expression in Sertoli cells via regulation of *E2f3*, also *in vivo*.

In summary, *Rb* is crucial for the maintenance of cell cycle quiescence in adult mouse Sertoli cells and the main function of RB is to inhibit transcription factor E2F3. Without functional RB, E2F3 can drive adult Sertoli cells to resume proliferation. As a

result, Sertoli cells are unable to support the spermatogonial stem cell niche, spermatogenesis and blood–testis barrier integrity, which ultimately leads to infertility. This study elucidates the significance of cell cycle status for the maintenance of Sertoli cell function and uncovers the critical contribution of the RB–E2F3 pathway in this process. Mature Sertoli cells need to remain mitotically quiescent to be able to carry out their function as supporters of spermatogenesis.

MATERIALS AND METHODS

Animals

Animals (strains and sources listed below) were housed under environmentally controlled conditions (12 h light:12 h darkness; temperature 21±1°C) in the animal facility of the University of Turku. They were fed soy-free RM-3 (E) mouse chow (Special Diet Services, Essex, UK) and tap water *ad libitum*. All procedures were carried out according to the institutional and ethical policies of the University of Turku and approved by the local ethics committee on animal experimentation.

Animals were euthanized by carbon dioxide inhalation and cervical dislocation. For mRNA and protein expression analysis of the target of study, control male mice were euthanized at P6, P10, P20 and P40. For the SC-*E2f3*$^{-/-}$ study, male mice were euthanized at a young adult age (2 months old) and after aging (5 months old). For the SC-*Rb*$^{-/-}$*E2f3*$^{-/-}$ study, 2.5 months was chosen as the primary experimental timepoint, because at this age a clear disruptive phenotype could be seen in the SC-*Rb*$^{-/-}$*E2f3*$^{+/+}$ testes, which enabled assessing the rescue effect of *E2f3* loss.

Breeding and genotyping of the mouse strains

We used three established transgenic mouse lines: a transgenic mouse line expressing Cre recombinase under the control of the anti-Müllerian hormone (*Amh*) promoter, selectively in Sertoli cells [B6; SJL-Plekha5Tg (*Amh*-cre) 1Flor/Orl] (generously provided by Dr Florian Guillou, French National Institute for Agricultural Research, Paris, France) (Lécureuil et al., 2002), *Rb*-floxed (*Rb*$^{flox/flox}$) (generously provided by Dr Anton Berns, The Netherlands Cancer Institute, Amsterdam, The Netherlands) (Marino et al., 2000; Vooijs et al., 1998) and *E2f3*-floxed (*E2f3*$^{flox/flox}$) mouse line (*E2f3*$^{tm1.1Gle}$) (generously provided by Prof. Gustavo Leone, Ohio State University, Ohio, USA) (Wu et al., 2001). The *E2f3*-floxed mice were obtained as cryopreserved sperm, and the IVF for the strain rederivation was performed by the transgenic core unit of University of Oulu using C57BL/6 oocytes. Primers for genotyping PCR were: *Amh*-cre, Cre26 (5′-CCTGGAAAATGCTTCTGTCCG-3′) and Cre36 (5′-CAGGGTGTTATAAGCAATCCC-3′), which amplify a 400 bp Cre product; *E2f3*-floxed allele, *E2f3* A (5′-GTGGCTGGAAGGG-TGCCAAG-3′), *E2f3* B (5′-TGAATCATGGACAGAGCCAGG-3′) and *E2f3* C (5′-GATTGATTCTGGGTTGTCAGG-3′), which amplify a 250 bp fragment for *E2f3*-floxed allele and a 200 bp fragment for *E2f3*-WT allele (Wu et al., 2001); *Rb*-floxed allele, *Rb*lox1 (5′-GGCGTGTGCCCA-TCAATG-3′) and *Rb*lox2 (5′-AACTCAAGGGAGACCTG-3′), which amplify a 700 bp fragment for *Rb*-floxed allele and a 650 bp fragment for *Rb*-WT allele.

Fertility

Fertility testing was conducted by breeding four males per experimental group with four C57Bl6/NCrl females for 24 h (or 48 h if a copulatory plug was not observed after 24 h). For the SC-*E2f3*$^{-/-}$ strain the test was performed at the ages of 2 and 5 months. For the SC-*Rb*$^{-/-}$*E2f3*$^{-/-}$ strain a single time point of 2.5 months was used in order to target the same age as that primarily analyzed for adults in the previous publication on SC-*Rb*$^{-/-}$*E2f3*$^{+/+}$ animals in the hybrid genetic background (Rotgers et al., 2014). The number and sex ratio of the pups was recorded and displayed as mean±s.e.m. pups per litter. Statistical testing was performed using paired *t*-test for the SC-*E2f3*$^{-/-}$ strain and one-way ANOVA followed by Tukey's test for the SC-*Rb*$^{-/-}$*E2f3*$^{-/-}$ strain.

Quantitative analysis of testicular cell populations by flow cytometry

Testis tissue from five adult litter-mate SC-*E2f3*$^{-/-}$ (cre+; *E2f3*$^{flox/flox}$) and control (cre−; *E2f3*$^{flox/flox}$) mice (2 and 5 months) and SC-*Rb*$^{-/-}$ *E2f3*$^{-/-}$ (cre+; *Rb*$^{flox/flox}$; *E2f3*$^{flox/flox}$), SC-*Rb*$^{-/-}$ *E2f3*$^{+/-}$ (cre+; *Rb*$^{flox/flox}$; *E2f3*$^{flox/wt}$), SC-*Rb*$^{-/-}$*E2f3*$^{+/+}$ (cre+; *Rb*$^{flox/flox}$; *E2f3*$^{wt/wt}$) and control (cre−; *Rb*$^{flox/flox}$; *E2f3*$^{flox/flox}$) mice (2.5 months) were analyzed. Briefly, testes were decapsulated and weighed to 10 mg per sample. Tissue was cut using McPherson–Vannas scissors and enzymatically digested with 1 mg/ml collagenase/dispase (10269638001; Roche), 1 mg/ml hyaluronidase (H3506; Sigma-Aldrich), 1 mg/ml DNase1 (DN-25; Sigma-Aldrich). Cell suspensions were filtered through 35-µm pore size filters (352235; BD Falcon) and subsequently fixed and permeabilized using 4% paraformaldehyde and 90% methanol. To evaluate the testicular cell composition and meiotic progression, DNA staining was performed. Additionally, for exclusion of dead cells in our analysis, LIVE/DEAD Near-IR staining (L-10119; Invitrogen, Thermo Fisher Scientific) was performed prior to fixation. A fixed volume of samples was analyzed using a BD LSRII (Becton Dickinson) equipped with a high-throughput sampler (HTS) in 96-well plate format. A 488 nm laser was used for excitation of propidium iodide and emission wavelengths were collected with a 575/26-nm band pass filter. Analyses were performed with the noncommercial Flowing Software v2.5 (Perttu Terho, Turku Centre for Biotechnology, Finland; www.flowingsoftware.com) as previously described in detail (Rotgers et al., 2015).

Serum gonadotrophin and intratesticular testosterone assays

Serum was collected from 2.5-month-old control, SC-*Rb*$^{-/-}$*E2f3*$^{+/+}$, SC-*Rb*$^{-/-}$*E2f3*$^{+/-}$ and SC-*Rb*$^{-/-}$*E2f3*$^{-/-}$ males and 2- and 5-month-old controls and SC-*E2f3*$^{-/-}$ males (n=8/group). Serum FSH and LH were analyzed using immunofluorometric assay (IFMA) (Delfia, Wallac Oy, Turku, Finland). For the FSH assay 65 µl of serum was diluted to 1:5. The sensitivity of the assay was 0.1 µg/l (van Casteren et al., 2000). For the LH assay, 25 µl of serum was used. The sensitivity of the assay was 0.03 µg/l in 25 µl (Haavisto et al., 1993). For the intratesticular testosterone assay, pieces of testicular tissue were weighed and homogenized in PBS. 200 µl of the homogenate was extracted twice with diethyl ether and dried through evaporation. The residues were reconstituted in PBS with 0.1% BSA and measured using a radio-immunoassay kit (TESTO-CT2; Cisbio Bioassays, Codolet, France). The analytical detection limit was better than 0.1 nmol/l and functional detection limit is approximately 0.3 nmol/l. The intra-assay and inter-assay coefficients of variation for testosterone were 10.5% and 17.3% in the SC-*E2f3*$^{-/-}$ analysis and 10.8% and 19.3% in the SC-*Rb*$^{-/-}$*E2f3*$^{-/-}$. All serum samples within an analysis were assayed at the same time using specific antiserum and radiolabeled hormones diluted the same day.

Histology

For the histological analysis the testes were fixed in Bouin's fixative overnight at room temperature. After serial washes in ethanol followed by dehydration, the testes were embedded in paraffin. Sections at 4 µm thick were cut from the testes and every tenth section was collected for the analysis. The sections were stained with periodic acid–Schiff (PAS) and imaged using Pannoramic 250 slide scanner with the 20× objective (3DHISTECH Ltd).

Immunohistochemical sample processing

Testes were fixed overnight in 4% paraformaldehyde (Electron Microscopy Sciences) and embedded in paraffin. Sections at 4 µm thick were cut. When the cell counts were quantified, every tenth section was chosen for the analysis. The analyzed sections were ten sections apart to avoid reanalyzing the same cells on each section. The TUNEL and SOX9 assay was conducted as described previously (Rotgers et al., 2014). The antibodies used and their dilutions are summarized in Table S1, except where indicated otherwise.

Germ cell apoptosis was only quantified from stage VII–VIII seminiferous tubule cross-sections to increase the sensitivity in detecting excess apoptosis, since there is a very low level of apoptosis in these stages in normal testes (Yan et al., 2000). Intratubular TUNEL-positive SOX9-negative cells were classified as apoptotic germ cells. For SC-*Rb*$^{-/-}$*E2f3*$^{+/+}$ testes, random tubule sections were chosen for the analysis because it was not possible to identify seminiferous tubule stages VII–VIII in the absence of spermatids.

Sertoli cell proliferation was quantified from SOX9- and KI67-stained testicular sections. The number of double-positive Sertoli cells for two hundred Sertoli cells on a section was quantified. Three sections, each 50 µm apart, were quantified for each animal.

p130 and p107 were detected on testicular sections with a Novolink chromogenic immunohistochemistry kit (Leica) according to the manufacturer's instructions. After detecting the signal with DAB, samples were counterstained using Mayer's hematoxylin, dehydrated and embedded with Pertex. The slides were imaged using a Pannoramic MIDI FL slide scanner with a 20× Plan Apochromat objective (Zeiss).

RNA *in situ* hybridization

An Advanced Cell Diagnostics (ACD) RNAscope 2-plex chromogenic assay kit (ACD-320700,) was used to detect *E2f3a* and *E2f3ab* mRNA on mouse PFA-fixed paraffin-embedded mouse testicular samples. Custom probes were designed by ACD for the detection of the *E2f3* isoforms. In addition, the positive (ACD-310751) and negative (ACD-320741) control probes accompanying the kit were used. *E2f3a* mRNA signal was detected using the red Vulcan Fast Red chromogen provided in the kit. The *E2f3ab* signal was detected using an alternative black chromogen (provided as a custom reagent by ACD). The assay was run according to the manufacturer's instructions with some modifications. The slides were incubated in the 'pretreat 2' reagent for 15 min and for 20 min in 'pretreat 3'. Mayer's hematoxylin was used as a counterstain and water at pH 11 was used to induce blue color in the hematoxylin stain. The samples were air-dried at room temperature and mounted using Ecomount. For the RNA *in situ* hybridization coupled to immunohistochemistry (IHC) of vimentin, the slides were processed as described above until the chromogenic reaction for both of the probes was ready. Then they were incubated with 5% horse serum in TBS followed by an overnight incubation with the primary antibody [anti-vimentin (VIM) diluted 1:3000 in 5% horse serum in TBS] at +4°C. Residual HRP activity was blocked by an incubation in 3% hydrogen peroxide in water. The primary antibody was detected using a biotinylated horse anti-rabbit antibody (1:500 in 5% horse serum in TBS) followed by Vector ABC-HRP kit. HIGHDEF yellow IHC chromogen (HRP) (Enzo Life Sciences) was used to visualize the vimentin staining. The slides were air-dried at room temperature and mounted using Ecomount. The slides were imaged using a Pannoramic MIDI FL slide scanner with a 40×/Korr 0.95 Plan Apochromat objective (Zeiss) using an extended focus to better visualize the RNAScope signal.

RNA isolation and qRT-PCR

Total RNA was isolated from P10 (control only) and adult mouse (control, SC-$Rb^{-/-}E2f3^{+/+}$, SC-$Rb^{-/-}E2f3^{+/-}$ and SC-$Rb^{-/-}E2f3^{-/-}$) testes (n=4–5/group) using the RNeasy Mini kit (74104; Qiagen). Subsequently, the obtained total RNA was treated with RNase-free DNase (79254; Qiagen) and purified using the RNeasy MinElute Clean-up kit (74204; Qiagen). RNA quality and concentration were determined using Nanodrop.

Targeted RNA sequencing

A custom assay panel was designed for the TruSeq targeted RNA sequencing (Illumina) (Table S3). The panel consisted of a selection of testicular cell type marker genes and known cell cycle-related genes. In addition, putative E2F target genes were chosen both from the literature (Bracken et al., 2004) and by comparing the differentially expressed genes in juvenile SC-$Rb^{-/-}E2f3^{+/+}$ testis (Rotgers et al., 2014) and adult Sertoli cells (Nalam et al., 2009) to ChIP-on-chip data on *E2f3* and *E2f1* target genes from murine and human cells (Asp et al., 2009; Cao et al., 2011) and overlapping genes were selected to be added to the panel. For the assay, whole testis mRNA was extracted from animals of various genotypes and ages as described above. For a detailed experimental setup see Table S2.

The library preparation and sequencing were performed at the Finnish Functional Genomics Centre (FFGC, Turku, Finland). Prior to the library preparation, the quality of the total RNA samples was ensured using an Agilent Bioanalyzer 2100 and an Advanced Analytical Fragment Analyzer. Total RNA samples were pure, intact and all samples had similar quality. Bioanalyzer RNA integrity number (RIN) values were >9.0. 50 ng of RNA was taken for the library preparation. Library preparation was done according to the Illumina TruSeq Targeted RNA Expression Guide (15034665). The high quality of the libraries was confirmed using an Advanced Analytical Fragment Analyzer. The libraries were normalized and pooled for the automated cluster preparation, which was carried out using an Illumina MiSeq instrument. The 44 libraries were pooled into a single pool. The samples were sequenced in a single run on the Illumina MiSeq instrument using v2 sequencing chemistry. Single-read sequencing with 1×50 bp read length was used, followed by 6 bp+8 bp dual index run. Technical quality of the MiSeq run was good and the cluster amount was as expected. Greater than 90% of all bases above Q30 was requested.

The results were submitted to the Illumina BaseSpace data management and analysis interphase. The TruSeq Targeted RNA sequencing application v1.0 was used to analyze differential expression of the transcripts in the experimental groups. Briefly, the depth of sequencing between samples was estimated and the expression levels for each replicate were normalized based on the total number of aligned reads. The normalized transcript abundance was modeled by a negative binomial distribution model and this model was used to derive a *P*-value for the differential expression of each transcript. Finally, the application corrected for multiple hypothesis testing by adjusting the *P*-value for false discovery rate (FDR) using the Benjamini–Hochberg method. *Hprt*, *Rpl19* and *Ppia* were used as reference genes for normalization during the analysis. The gene expression results are visualized as fold changes of the pairwise comparisons between control and experimental groups.

Acknowledgements

We want to thank Prof. Gustavo Leone (Ohio State University, Ohio, USA) for generously providing us with the *E2f3*-floxed (*E2f3*$^{flox/flox}$) mouse line (*E2f3*$^{tm1.1Gle}$). We are grateful to Erica Nyman for her expertise in histological sample preparation and to Mrs Taina Kirjonen for conducting hormone assays.

Competing interests

The authors declare no competing or financial interests.

Author contributions

Conceptualization: E.R., M.N., J.T.; Methodology: E.R., S.C.-M., J.T.; Software: S.C.-M.; Investigation: E.R., S.C.-M., M.N., J.T.; Resources: J.T.; Data curation: E.R., S.C.-M., J.T.; Writing - original draft: E.R.; Writing - review & editing: S.C.-M., M.N., J.T.; Visualization: E.R., S.C.-M., M.N.; Supervision: J.T.; Funding acquisition: J.T.

Funding

This work was funded by Academy of Finland, Sigrid Juséliuksen Säätiö, Turun Yliopisto [University of Turku Graduate School (UTUGS)], Novo Nordisk Fonden, Kirsten og Freddy Johansens Fond, Jalmari ja Rauha Ahokkaan Säätiö and Turun Yliopistollinen Keskussairaala (Turku University Hospital) special research grants.

Data availability

Data from the targeted RNA sequencing have been deposited in GEO under the accession number GSE133756.

Supplementary information

Supplementary information available online at
http://jcs.biologists.org/lookup/doi/10.1242/jcs.229849.supplemental

References

Adams, M. R., Sears, R., Nuckolls, F., Leone, G. and Nevins, J. R. (2000). Complex transcriptional regulatory mechanisms control expression of the E2F3 locus. *Mol. Cell. Biol.* **20**, 3633-3639. doi:10.1128/MCB.20.10.3633-3639.2000

Ahmed, E. A., Barten-van Rijbroek, A. D., Kal, H. B., Sadri-Ardekani, H., Mizrak, S. C., van Pelt, A. M. and de Rooij, D. G. (2009). Proliferative activity in vitro and DNA repair indicate that adult mouse and human Sertoli cells are not terminally differentiated, quiescent cells. *Biol. Reprod.* **80**, 1084-1091. doi:10.1095/biolreprod.108.071662

Archambeault, D. R. and Yao, H. H.-C. (2014). Loss of smad4 in Sertoli and Leydig cells leads to testicular dysgenesis and hemorrhagic tumor formation in mice. *Biol. Reprod.* **90**, 62. doi:10.1095/biolreprod.113.111393

Asp, P., Acosta-Alvear, D., Tsikitis, M., van Oevelen, C. and Dynlacht, B. D. (2009). E2f3b plays an essential role in myogenic differentiation through isoform-specific gene regulation. *Genes Dev.* **23**, 37-53. doi:10.1101/gad.1727309

Barakat, B., O'Connor, A. E., Gold, E., de Kretser, D. M. and Loveland, K. L. (2008). Inhibin, activin, follistatin and FSH serum levels and testicular production are highly modulated during the first spermatogenic wave in mice. *Reproduction* **136**, 345-359. doi:10.1530/REP-08-0140

Bracken, A. P., Ciro, M., Cocito, A. and Helin, K. (2004). E2F target genes: unraveling the biology. *Trends Biochem. Sci.* **29**, 409-417. doi:10.1016/j.tibs.2004.06.006

Bremner, W. J., Millar, M. R., Sharpe, R. M. and Saunders, P. T. (1994). Immunohistochemical localization of androgen receptors in the rat testis: Evidence for stage-dependent expression and regulation by androgens. *Endocrinology* **135**, 1227-1234. doi:10.1210/endo.135.3.8070367

Cao, A. R., Rabinovich, R., Xu, M., Xu, X., Jin, V. X. and Farnham, P. J. (2011). Genome-wide analysis of transcription factor E2F1 mutant proteins reveals that N- and C-terminal protein interaction domains do not participate in targeting E2F1 to the human genome. *J. Biol. Chem.* **286**, 11985-11996. doi:10.1074/jbc.M110.217158

Capel, B. (2017). Vertebrate sex determination: evolutionary plasticity of a fundamental switch. *Nat. Rev. Genet.* **18**, 675-689. doi:10.1038/nrg.2017.60

Carrano, A. C., Eytan, E., Hershko, A. and Pagano, M. (1999). SKP2 is required for ubiquitin-mediated degradation of the CDK inhibitor p27. *Nat. Cell Biol.* **1**, 193-199. doi:10.1038/12013

Chen, H.-Z., Tsai, S.-Y. and Leone, G. (2009). Emerging roles of E2Fs in cancer: an exit from cell cycle control. *Nat. Rev. Cancer.* **9**, 785-797. doi:10.1038/nrc2696

Chong, J.-L., Wenzel, P. L., Sáenz-Robles, M. T., Nair, V., Ferrey, A., Hagan, J. P., Gomez, Y. M., Sharma, N., Chen, H.-Z., Ouseph, M. et al. (2009). E2f1-3 switch from activators in progenitor cells to repressors in differentiating cells. *Nature* **462**, 930-934. doi:10.1038/nature08677

Danielian, P. S., Friesenhahn, L. B., Faust, A. M., West, J. C., Caron, A. M., Bronson, R. T. and Lees, J. A. (2008). E2f3a and E2f3b make overlapping but different contributions to total E2f3 activity. *Oncogene* **27**, 6561-6570. doi:10.1038/onc.2008.253

De Gendt, K., Swinnen, J. V., Saunders, P. T. K., Schoonjans, L., Dewerchin, M., Devos, A., Tan, K., Atanassova, N., Claessens, F., Lecureuil, C. et al. (2004). A Sertoli cell-selective knockout of the androgen receptor causes spermatogenic arrest in meiosis. *Proc. Natl. Acad. Sci. USA* **101**, 1327-1332. doi:10.1073/pnas.0308114100

El-Darwish, K. S., Parvinen, M. and Toppari, J. (2006). Differential expression of members of the E2F family of transcription factors in rodent testes. *Reprod. Biol. Endocrinol.* **4**, 63. doi:10.1186/1477-7827-4-63

Gow, A., Southwood, C. M., Li, J. S., Pariali, M., Riordan, G. P., Brodie, S. E., Danias, J., Bronstein, J. M., Kachar, B. and Lazzarini, R. A. (1999). CNS myelin and Sertoli cell tight junction strands are absent in Osp/Claudin-11 null mice. *Cell* **99**, 649-659. doi:10.1016/S0092-8674(00)81553-6

Greenspan, L. J. and Matunis, E. L. (2018). Retinoblastoma intrinsically regulates niche cell quiescence, identity, and niche number in the adult drosophila testis. *Cell. Rep.* **24**, 3466-3476.e8. doi:10.1016/j.celrep.2018.08.083

Gromoll, J., Wessels, J., Rosiepen, G., Brinkworth, M. H. and Weinbauer, G. F. (1997). Expression of mitotic cyclin B1 is not confined to proliferating cells in the rat testis. *Biol. Reprod.* **57**, 1312-1319. doi:10.1095/biolreprod57.6.1312

Guo, Q., Kumar, T. R., Woodruff, T., Hadsell, L. A., DeMayo, F. J. and Matzuk, M. M. (1998). Overexpression of mouse follistatin causes reproductive defects in transgenic mice. *Mol. Endocrinol.* **12**, 96-106. doi:10.1210/mend.12.1.0053

Haavisto, A. M., Pettersson, K., Bergendahl, M., Perheentupa, A., Roser, J. F. and Huhtaniemi, I. (1993). A supersensitive immunofluorometric assay for rat luteinizing hormone. *Endocrinology* **132**, 1687-1691. doi:10.1210/endo.132.4.8462469

He, Y., Armanious, M. K., Thomas, M. J. and Cress, W. D. (2000). Identification of E2F-3B, an alternative form of E2F-3 lacking a conserved N-terminal region. *Oncogene* **19**, 3422-3433. doi:10.1038/sj.onc.1203682

Julian, L. M., Vandenbosch, R., Pakenham, C. A., Andrusiak, M. G., Nguyen, A. P., McClellan, K. A., Svoboda, D. S., Lagace, D. C., Park, D. S., Leone, G. et al. (2013). Opposing regulation of Sox2 by cell-cycle effectors E2f3a and E2f3b in neural stem cells. *Cell. Stem Cell.* **12**, 440-452. doi:10.1016/j.stem.2013.02.001

Kashimada, K. and Koopman, P. (2010). Sry: the master switch in mammalian sex determination. *Development* **137**, 3921-3930. doi:10.1242/dev.048983

Kong, L.-J., Chang, J. T., Bild, A. H. and Nevins, J. R. (2007). Compensation and specificity of function within the E2F family. *Oncogene* **26**, 321-327. doi:10.1038/sj.onc.1209817

Lécureuil, C., Fontaine, I., Crepieux, P. and Guillou, F. (2002). Sertoli and granulosa cell-specific Cre recombinase activity in transgenic mice. *Genesis* **33**, 114-118. doi:10.1002/gene.10100

Leone, G., Nuckolls, F., Ishida, S., Adams, M., Sears, R., Jakoi, L., Miron, A. and Nevins, J. R. (2000). Identification of a novel E2F3 product suggests a mechanism for determining specificity of repression by Rb proteins. *Mol. Cell. Biol.* **20**, 3626-3632. doi:10.1128/MCB.20.10.3626-3632.2000

Ling, N., Ying, S.-Y., Ueno, N., Shimasaki, S., Esch, F., Hotta, F. E. M. and Guillemin, R. (1986). A homodimer of the beta-subunits of inhibin A stimulates the secretion of pituitary follicle stimulating hormone. *Biochem. Biophys. Res. Commun.* **138**, 1129-1137. doi:10.1016/S0006-291X(86)80400-4

Manova, K., Nocka, K., Besmer, P. and Bachvarova, R. F. (1990). Gonadal expression of c-kit encoded at the W locus of the mouse. *Development* **110**, 1057-1069.

Marino, S., Vooijs, M., van Der Gulden, H., Jonkers, J. and Berns, A. (2000). Induction of medulloblastomas in p53-null mutant mice by somatic inactivation of rb in the external granular layer cells of the cerebellum. *Genes Dev.* **14**, 994-1004.

Martinerie, L., Manterola, M., Chung, S. S. W., Panigrahi, S. K., Weisbach, M., Vasileva, A., Geng, Y., Sicinski, P. and Wolgemuth, D. J. (2014). Mammalian E-type cyclins control chromosome pairing, telomere stability and CDK2 localization in male meiosis. *PLoS Genet.* **10**, e1004165. doi:10.1371/journal.pgen.1004165

Matzuk, M. M., Finegold, M. J., Su, J.-G. J., Hsueh, A. J. W. and Bradley, A. (1992). Alpha-inhibin is a tumour-suppressor gene with gonadal specificity in mice. *Nature* **360**, 313-319. doi:10.1038/360313a0

Mazaud-Guittot, S., Meugnier, E., Pesenti, S., Wu, X., Vidal, H., Gow, A. and Le Magueresse-Battistoni, B. (2010). Claudin 11 deficiency in mice results in loss of the Sertoli cell epithelial phenotype in the testis. *Biol. Reprod.* **82**, 202-213. doi:10.1095/biolreprod.109.078907

Meng, J., Holdcraft, R. W., Shima, J. E., Griswold, M. D. and Braun, R. E. (2005). Androgens regulate the permeability of the blood-testis barrier. *Proc. Natl. Acad. Sci. USA* **102**, 16696-16700. doi:10.1073/pnas.0506084102

Mirza, M., Hreinsson, J., Strand, M.-L., Hovatta, O., Söder, O., Philipson, L., Pettersson, R. F. and Sollerbrant, K. (2006). Coxsackievirus and adenovirus receptor (CAR) is expressed in male germ cells and forms a complex with the differentiation factor JAM-C in mouse testis. *Exp. Cell Res.* **312**, 817-830. doi:10.1016/j.yexcr.2005.11.030

Moberg, K., Starz, M. A. and Lees, J. A. (1996). E2F-4 switches from p130 to p107 and pRB in response to cell cycle reentry. *Mol. Cell. Biol.* **16**, 1436-1449. doi:10.1128/MCB.16.4.1436

Müller, H., Bracken, A. P., Vernell, R., Moroni, M. C., Christians, F., Grassilli, E., Prosperini, E., Vigo, E., Oliner, J. D. and Helin, K. (2001). E2Fs regulate the expression of genes involved in differentiation, development, proliferation, and apoptosis. *Genes Dev.* **15**, 267-285. doi:10.1101/gad.864201

Nakamura, T., Takio, K., Eto, Y., Shibai, H., Titani, K. and Sugino, H. (1990). Activin-binding protein from rat ovary is follistatin. *Science* **247**, 836-838. doi:10.1126/science.2106159

Nalam, R. L., Andreu-Vieyra, C., Braun, R. E., Akiyama, H. and Matzuk, M. M. (2009). Retinoblastoma protein plays multiple essential roles in the terminal differentiation of Sertoli cells. *Mol. Endocrinol.* **23**, 1900-1913. doi:10.1210/me.2009-0184

Polyak, K., Lee, M.-H., Erdjument-Bromage, H., Koff, A., Roberts, J. M., Tempst, P. and Massagué, J. (1994). Cloning of p27Kip1, a cyclin-dependent kinase inhibitor and a potential mediator of extracellular antimitogenic signals. *Cell* **78**, 59-66. doi:10.1016/0092-8674(94)90572-X

Ranganathan, S., Ganguly, A. K. and Datta, K. (1994). Evidence for presence of hyaluronan binding protein on spermatozoa and its possible involvement in sperm function. *Mol. Reprod. Dev.* **38**, 69-76. doi:10.1002/mrd.1080380112

Rebourcet, D., Darbey, A., Monteiro, A., Soffientini, U., Tsai, Y. T., Handel, I., Pitetti, J.-L., Nef, S., Smith, L. B. and O'Shaughnessy, P. J. (2017). Sertoli cell number defines and predicts germ and Leydig cell population sizes in the adult mouse testis. *Endocrinology* **158**, 2955-2969. doi:10.1210/en.2017-00196

Robertson, D. M., Foulds, L. M., Leversha, L., Morgan, F. J., Hearn, M. T. W., Burger, H. G., Wettenhall, R. E. H. and de Kretser, D. M. (1985). Isolation of inhibin from bovine follicular fluid. *Biochem. Biophys. Res. Commun.* **126**, 220-226. doi:10.1016/0006-291X(85)90594-7

Rotgers, E., Rivero-Müller, A., Nurmio, M., Parvinen, M., Guillou, F., Huhtaniemi, I., Kotaja, N., Bourguiba-Hachemi, S. and Toppari, J. (2014). Retinoblastoma protein (RB) interacts with E2F3 to control terminal differentiation of Sertoli cells. *Cell. Death Dis.* **5**, e1274. doi:10.1038/cddis.2014.232

Rotgers, E., Cisneros-Montalvo, S., Jahnukainen, K., Sandholm, J., Toppari, J. and Nurmio, M. (2015). A detailed protocol for a rapid analysis of testicular cell populations using flow cytometry. *Andrology* **3**, 947-955. doi:10.1111/andr.12066

Smith, B. E. and Braun, R. E. (2012). Germ cell migration across Sertoli cell tight junctions. *Science* **338**, 798-802. doi:10.1126/science.1219969

Spiller, C. M., Wilhelm, D. and Koopman, P. (2010). Retinoblastoma 1 protein modulates XY germ cell entry into G1/G0 arrest during fetal development in mice. *Biol. Reprod.* **82**, 433-443. doi:10.1095/biolreprod.109.078691

Sridharan, S., Simon, L., Meling, D. D., Cyr, D. G., Gutstein, D. E., Fishman, G. I., Guillou, F. and Cooke, P. S. (2007). Proliferation of adult Sertoli cells following conditional knockout of the gap junctional protein GJA1 (connexin 43) in mice. *Biol. Reprod.* **76**, 804-812. doi:10.1095/biolreprod.106.059212

Tarulli, G. A., Stanton, P. G., Lerchl, A. and Meachem, S. J. (2006). Adult Sertoli cells are not terminally differentiated in the djungarian hamster: effect of FSH on proliferation and junction protein organization. *Biol. Reprod.* **74**, 798-806. doi:10.1095/biolreprod.105.050450

Tarulli, G. A., Stanton, P. G. and Meachem, S. J. (2012). Is the adult Sertoli cell terminally differentiated? *Biol. Reprod.* **87**, 13, 1-11. doi:10.1095/biolreprod.111.095091

Tsai, S.-Y., Opavsky, R., Sharma, N., Wu, L., Naidu, S., Nolan, E., Feria-Arias, E., Timmers, C., Opavska, J., de Bruin, A. et al. (2008). Mouse development with a single E2F activator. *Nature* **454**, 1137-1141. doi:10.1038/nature07066

Ungewitter, E. K. and Yao, H. H.-C. (2013). How to make a gonad: cellular mechanisms governing formation of the testes and ovaries. *Sex. Dev.* **7**, 7-20. doi:10.1159/000338612

van Casteren, J. I. J., Schoonen, W. G. E. J. and Kloosterboer, H. J. (2000). Development of time-resolved immunofluorometric assays for rat follicle-

stimulating hormone and luteinizing hormone and application on sera of cycling rats. *Biol. Reprod.* **62**, 886-894. doi:10.1095/biolreprod62.4.886

Vergouwen, R. P. F. A., Jacobs, S. G. P. M., Huiskamp, R., Davids, J. A. G. and de Rooij, D. G. (1991). Proliferative activity of gonocytes, Sertoli cells and interstitial cells during testicular development in mice. *J. Reprod. Fertil.* **93**, 233-243. doi:10.1530/jrf.0.0930233

Vooijs, M., van der Valk, M., te Riele, H. and Berns, A. (1998). Flp-mediated tissue-specific inactivation of the retinoblastoma tumor suppressor gene in the mouse. *Oncogene* **17**, 1-12. doi:10.1038/sj.onc.1202169

Wijayarathna, R. and de Kretser, D. M. (2016). Activins in reproductive biology and beyond. *Hum. Reprod. Update* **22**, 342-357. doi:10.1093/humupd/dmv058

Wu, L., Timmers, C., Maiti, B., Saavedra, H. I., Sang, L., Chong, G. T., Nuckolls, F., Giangrande, P., Wright, F. A., Field, S. J. et al. (2001). The E2F1-3 transcription factors are essential for cellular proliferation. *Nature* **414**, 457-462. doi:10.1038/35106593

Wu, R.-C., Jiang, M., Beaudet, A. L. and Wu, M.-Y. (2013). ARID4A and ARID4B regulate male fertility, a functional link to the AR and RB pathways. *Proc. Natl. Acad. Sci. USA* **110**, 4616-4621. doi:10.1073/pnas.1218318110

Yamamoto, T., Nakayama, Y. and Abé, S.-I. (2001). Mammalian follicle-stimulating hormone and insulin-like growth factor I (IGF-I) up-regulate IGF-I gene expression in organ culture of newt testis. *Mol. Reprod. Dev.* **60**, 56-64. doi:10.1002/mrd.1061

Yan, W., Suominen, J., Samson, M., Jegou, B. and Toppari, J. (2000). Involvement of Bcl-2 family proteins in germ cell apoptosis during testicular development in the rat and pro-survival effect of stem cell factor on germ cells in vitro. *Mol. Cell. Endocrinol.* **165**, 115-129. doi:10.1016/S0303-7207(00)00257-4

Zheng, N., Fraenkel, E., Pabo, C. O. and Pavletich, N. P. (1999). Structural basis of DNA recognition by the heterodimeric cell cycle transcription factor E2F-DP. *Genes Dev.* **13**, 666-674. doi:10.1101/gad.13.6.666

Ziebold, U., Reza, T., Caron, A. and Lees, J. A. (2001). E2F3 contributes both to the inappropriate proliferation and to the apoptosis arising in Rb mutant embryos. *Genes Dev.* **15**, 386-391. doi:10.1101/gad.858801

Ziebold, U., Lee, E. Y., Bronson, R. T. and Lees, J. A. (2003). E2F3 loss has opposing effects on different pRB-deficient tumors, resulting in suppression of pituitary tumors but metastasis of medullary thyroid carcinomas. *Mol. Cell. Biol.* **23**, 6542-6552. doi:10.1128/MCB.23.18.6542-6552.2003

Zimmermann, C., Stévant, I., Borel, C., Conne, B., Pitetti, J.-L., Calvel, P., Kaessmann, H., Jégou, B., Chalmel, F. and Nef, S. (2015). Research resource: the dynamic transcriptional profile of Sertoli cells during the progression of spermatogenesis. *Mol. Endocrinol.* **29**, 627-642. doi:10.1210/me.2014-1356